ISSN 1023－9855

胸腔醫學

Thoracic Medicine

The Official Journal of Taiwan Society of Pulmonary and Critical Care Medicine

Vol.29 No.3 April 2014

第二十九卷 第二期

中華民國一〇三年四月

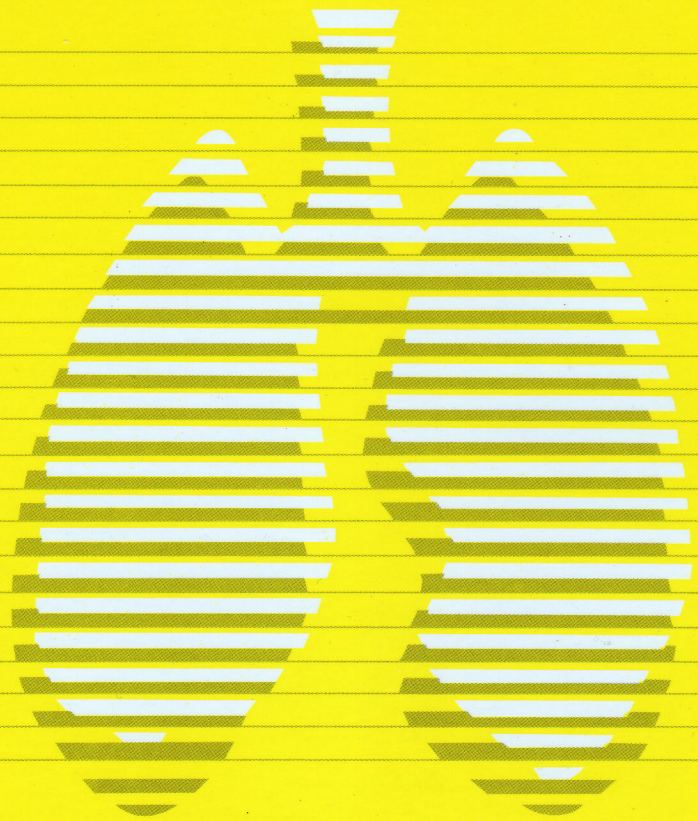

台灣胸腔暨重症加護醫學會

11217 台北市北投區石牌路二段201號

5.No.201, Sec. 2, Shipai Rd., Beitou District, Taipei City, Taiwan 11217, R.O.C.

ISSN 1023－9855

中華民國一〇三年四月　第二十九卷　第二期

ISSN 1023－9855

胸腔醫學

Thoracic Medicine

The Official Journal of Taiwan Society of Pulmonary and Critical Care Medicine

Vol.29 No.2 April 2014

原著

病例報告

中華民國一〇三年四月　第二十九卷　第二期

ISSN 1023－9855

Vol.29 No.2 April 2014

胸腔醫學

Thoracic Medicine

The Official Journal of Taiwan Society of Pulmonary and Critical Care Medicine

Orginial Articles

Case Reports

Robot-assisted Thoracic Surgery – Initial Experience at National Taiwan University Hospital

Shuenn-Wen Kuo, Pei-Ming Huang, Hsao-Hsun Hsu,
Jin-Shing Chen, Jang-Ming Lee

Purpose: We set up a prospective study to evaluate the efficacy of thoracic surgery using the da Vinci system in a single institution.

Methods: We prospectively enrolled patients who underwent robot-assisted thoracic surgery at Nation-al Taiwan University Hospital during the period February 2012 to July 2012. The procedures performed and patient numbers were thymothymectomy [1], lobectomy [10], esophagectomy [1] and excision of esophageal tumor [1].

Results: The median docking time of all procedures was 10.5 minutes (range, 4-21 minutes) and the median console time was 183 minutes (range, 72-327 minutes). No patient was converted to traditional laparoscopy or thoracoscopy, but 1 patient was converted to open surgery due to major bleeding. The postoperative morbidities included 1 prolonged air leak, 1 atrial fibrillation, and 1 worsening of myasthenia gravis. There was no mortality. The median drain tube duration was 3 days (range, 2-11 days), and the median hospital stay was 6 days (range, 4-19 days).

Conclusion: Robot-assisted thoracic surgery proved to be feasible and safe in our initial series in a learning curve setting. A longer follow-up period and randomized controlled trials are necessary to evaluate a potential benefit over open and conventional VATS approaches. ***(Thorac Med 2014; 29: 63-69)***

Key words: thoracic surgery, robot-assisted surgery

Introduction

At the beginning of the 1990s, the intro-duction of minimally invasive surgery led to revolutionary changes in the field of thoracic surgery. Minimally invasive surgery can be a feasible and safe alterna-tive to open surgery with additional benefits that include shorter hospital stay, decreased acute postop-erative pain, less release of inflammation mediators, better functional results, and enhanced recovery and tolerance of adjuvant therapy [1-3]. Nevertheless, because it is a technically demanding operation whose difficulties are compounded by the inherent disadvantages of video-assisted thoracic surgery (VATS)—rigid instruments re-

Departments of Surgery, National Taiwan University Hospital and National Taiwan University College of Medicine
Address reprint requests to: Dr. Jang-Ming Lee, Division of Thoracic Surgery, Department of Surgery, National Taiwan University Hospital, 7 Chung-San South Road, Taipei 100, Taiwan

stricting maneuverability, physiological tremor, and only 2-dimensional vision—most anatomic VATS are performed by a small number of highly experienced thoracoscopic surgeons [4]. A robotic surgical system has been developed to overcome some of these limitations. It has several theoretical advantages, including a 3-dimensional field of view, high definition imaging, more dexterous robotic arms with 7 degrees of freedom, filtration of physiological tremor, and greater comfort for the surgeon [5]. Several studies have shown efficacy and equivalent outcomes when com-pared with both VATS and open surgery [6-7].

In January 2012, a da Vinci system was introduced in our hospital, and we began setting up a program to perform thoracic operations for patients. We would like to share our initial experiences in this report.

Patients and Methods

Patients

The study population consisted of 13 elective patients who underwent robot-assisted thoracic sur-gery at National Taiwan University Hospital from February 2012 to July 2012. There were 10 males and 3 females with ages ranging from 30 to 78 years. We performed a variety of thoracoscopic opera-tions using the 4-arm da Vinci Surgical Robotic System (Intuitive Surgical, Sunnyvale, CA, USA). All of these operations have been routinely performed with traditional laparoscopy or thoracoscopy in our department, both before and after the introduction of robotic surgery. Patients were selected on the basis of being candidates for a minimally invasive approach. All of them were thoroughly informed about the novel approach and had given their written consent. Information regarding preoperative characteristics, operative details, hospital course, and postoperative follow-up were recorded at the time. Data specific to robotic surgery were also recorded:

(1) Docking time: time needed for the setup of the robotic system and positioning of the trocars until the surgeon sat at the console to start the robotic part of the procedure
(2) Console time: the overall duration of the operation by the surgeon using the robotic system

Set-up of the Operating Room

Equipment and personnel were positioned similarly to traditional thoracoscopic or laparoscopic surgery. All procedures were performed under general anesthesia. One-lung ventilation was achieved by use of a double-lumen endotracheal tube. A master–slave surgical cart was placed behind the patient's head. The right and left arms of the robot controlled the surgical instruments, and the endoscope was attached (high-resolution 30-degree endoscope) to the center arm. Trocars were positioned in a triangulation pattern at least 8 cm apart to allow adequate range of motion of the external arms. Minor modifications were otherwise necessary depending on the procedures performed. Standard stapling devices were used.

Results

There were 10 males and 3 females in this study population. Median age at surgery was 56 years (range, 30-78 years). The procedures included 1 radical thymothymectomy for myasthenia gravis with thymoma, 1 excision of esophageal leiomyoma, 1 esophagectomy with esophageal reconstruction for esophageal can-

cer, and 10 lobectomies for lung cancer. There was no mortality in our series. Demo-graphic data, diagnosis, complications, and duration of drain tube use and hospital stay are shown in detail in Table 1. Two (20%) of the 10 lung cancer patients were pathologic N2, and underwent neoad-juvant chemotherapy (No. 5) and neoadjuvant concurrent chemoradiation therapy (No. 13), respectively. The docking time generally decreased as familiarity with the system increased over time. However, the console time was relatively longer than in traditional thoracoscopic surgery because we were still within our learning curve. One intraoperative complication, pulmonary arterial laceration, occurred while using the endoscopic stapler for the bronchus. The lacerations were controlled successfully by endo-clips at first. But the following manipulation dislodged the clips and resulted in significant bleeding. We converted the operation to thoracotomy for pulmonary arterial repair (Table 2). There were 3 postoperative morbidities that were related to underlying diseases rather than the operation itself. Patient follow-up continued regularly on an outpatient basis in our department and no specific robotic surgery-related complication has been detected so far.

Table 1. Patients' Baseline Characteristics and Postoperative Outcome

Patient No.	Gender	Age	Diagnosis	Drain tube duration (d)	Length of hospital stay (d)	Morbidity
1	M	64	Lung cancer	2	4	No
2	M	78	Lung cancer	11	13	Prolonged air leak
3	M	56	Lung cancer	2	4	No
4	M	64	Esophageal leiomyoma	7	8	No
5	M	54	Lung cancer	2	5	No
6	M	41	Myasthenia gravis with thymoma	3	19	Worsening myasthenia gravis
7	F	76	Lung cancer	4	12	Atrial fibrillation
8	M	68	Lung cancer	3	5	No
9	F	51	Lung cancer	3	5	No
10	F	53	Lung cancer	3	6	No
11	M	66	Lung cancer	5	8	No
12	M	41	Esophageal cancer	4	16	No
13	M	30	Lung cancer	4	5	No

Table 2. Patients' Perioperative Outcome

Patient No.	Operative Method	Docking time (min)	Console time (min)	Blood loss (ml)	Transfusion	Intraoperative complication	Conversion
1	RLL lobectomy	20	161	100	No	No	No
2	RUL lobectomy	21	203	200	No	No	No
3	LUL lobectomy	18	169	400	No	No	No
4	Tumor excision	10	72	<50	No	No	No
5	RML lobectomy	5	279	100	No	No	No
6	Radial thymothymectomy	10	176	150	No	No	No
7	LLL lobectomy	11	190	3000	Yes	Pulmonary arterial laceration	Converted to thoracotomy
8	RUL lobectomy	19	171	<50	No	No	No
9	LUL lobectomy	4	162	100	No	No	No
10	LUL proper lobectomy	15	210	100	No	No	No
11	LUL lobectomy	6	327	400	No	No	No
12	Esophagectomy with gastric tube reconstruction	8 (Thoracic part) 10 (Abdominal part)	223 (Thoracic part) 120 (Abdominal part)	300	No	No	No
13	LUL lobectomy	17	327	150	No	No	No

Discussion

Robotic surgery has inaugurated a new era in minimally invasive surgery with major potential changes concerning the concept and performance of surgery itself [5]. With regard to thoracic surgery, there are several reports in the literature demonstrating the safety and feasibility of robot-assisted lo-bectomy, thymectomy, and esophagectomy [6,8-10].

We started the robotic operation with the same indications as for traditional thoracoscopic or lap-aroscopic surgery, and used the 4-arm da Vinci system. So far, we have performed 1 radical thymo-thymectomy for myasthenia gravis with thymoma, 1 excision of esophageal leiomyoma, 1 esoph-agectomy with esophageal reconstruction for esophageal cancer, and

10 lobectomies for lung cancer. There was no mortality in our series. However, 1 of the lobectomies had to be converted to thora-cotomy because of pulmonary arterial laceration. This complication was not directly related to the robotic system. Therefore, we concluded that robotic surgery is both feasible and safe for use in the thoracic field, based on our initial experience.

While robotic operations are comparable to traditional thoracoscopic procedures in terms of duration of operation, overall hospital stay, use of postoperative analgesics, and short-term clinical outcome [11], the system presents its superiority in the physical separation of the surgeon from the patient, the elimination of tremors, articulation for multiple angles of approach, optional motion downscaling, and 3-dimensional stereoscopic imaging [12]. The combination of this processing and filtering provides surgeons an unparallel level of operative precision using an ergonomically com-fortable position with minimum fatigue. The enhanced magnification allows a clear distinction of the anatomic structures, minimizing the risk of damage. And, the motion-scaling system that translates large hand movements into precise surgical maneuvers facilitates safe dissection of these delicate anatomic structures.

The major advantages we experienced were a better degree of freedom of the hand-like articula-tion, with the ability to dissect small delicate structures in confined areas such as the subcarinal space and to perform intracorporeal suturing. During a VATS procedure, lymphadenectomy can be chal-lenging and some authors recommend a combined VATS plus video-assisted mediastinoscopic lym-phadenectomy approach to left-sided tumors to make a pretracheal and paratracheal dissection possible and to facilitate complete dissection of the subcarinal space [13]. The good dexterity of the robotic arms, together with the 3-dimensional vision, facilitates an anatomically precise and radical dissection of the mediastinal and hilar lymph nodes [14], especially for the dense nodes following chemotherapy or radiation therapy. In our series, there was no major bleeding during lymphadenectomy, and no chylothorax or recurrent nerve injury emerged during the postoperative period.

The main problem related to using the current robotic system, as extensively reported in the liter-ature, is the loss of tactile feedback (or haptics). This drawback may result in the breaking of a suture during knot tying or iatrogenic organ injury. Although needle capture and tissue suturing is quite easy with the robotic system compared with traditional thoracoscopic techniques, a high degree of experi-ence is required to avoid tissue damage owing to the exercise of extensive force.

Another disadvantage of the present robotic system is the high costs compared with conventional procedures [15]. This includes the initial capital investment for the main robotic unit, intraoperative robotic supplies plus the cost of all other instruments used, such as staplers and endo-bags, and the maintenance contract. In view of the total utilization and capital costs, there needs to be a high rate of utilization of the system to make this investment cost-effective; however, this unfortunately has not been true for most purchasing institutions. We believe and hope that costs may fall as the tech-nology matures, competing manufacturers enter the field, and more machines become available.

In conclusion, robot-assisted thoracic surgery is safe and feasible, with short-term outcomes comparable to published results using

video-assisted or open approaches. Although many lessons are still being learned, our initial experience with robotic surgery is highly encouraging and we believe that the robotic system will serve as a platform for further improvements in minimally invasive surgical technologies.

References

1. Flores RM, Park BJ, Dycoco J, *et al*. Lobectomy by video-assisted thoracic surgery (VATS) versus thoracotomy for lung cancer. J Thorac Cardiovasc Surg 2009; 138: 11-8.
2. Villamizar NR, Darrabie MD, Burfeind WR, *et al*. Thoracoscopic lobectomy is associated with lower morbidity compared with thoracotomy. J Thorac Cardiovasc Surg 2009; 138: 419-25.
3. Petersen RP, Pham D, Burfeind WR, *et al*. Thoracoscopic lobectomy facilitates the delivery of chemotherapy after resection for lung cancer. Ann Thorac Surg 2007; 83: 1245-9; discussion 1250.
4. Melfi FM, Mussi A: Robotically assisted lobectomy: learning curve and complications. Thorac Surg Clin 2008; 18: 289-95, vi-vii.
5. Cerfolio RJ, Bryant AS, Minnich DJ: Starting a robotic program in general thoracic surgery: why, how, and lessons learned. Ann Thorac Surg 2011; 91: 1729-36.
6. Augustin F, Bodner J, Wykypiel H, *et al*. Perioperative results of robotic lung lobectomy: summary of literature. Surg Endosc 2012; 26: 1190-1.
7. Park BJ, Melfi F, Mussi A, *et al*. Robotic lobectomy for non-small cell lung cancer (NSCLC): long-term oncologic results. J Thorac Cardiovasc Surg 2012; 143: 383-9.
8. Fernando HC, Erdem CC, Daly B, Shemin RJ: Robotic assisted thoracic surgery for resection of an esophageal cyst. Dis Esophagus 2006; 19: 509-11.
9. Rea F, Schiavon M, Di Chiara F, Marulli G: Single-institution experience on robot-assisted thoracoscopic operations for mediastinal diseases. Innovations (Phila) 2011; 6: 316-22.
10. Pardolesi A, Park B, Petrella F, *et al*. Robotic anatomic segmentectomy of the lung: technical aspects and initial results. Ann Thorac Surg 2012.
11. Jang HJ, Lee HS, Park SY, Zo JI: Comparison of the early robot-assisted lobectomy experience to video-assisted thoracic surgery lobectomy for lung cancer: a single-institution case series matching study. Innovations (Phila) 2011; 6: 305-10.
12. Ballantyne GH: The pitfalls of laparoscopic surgery: challenges for robotics and telerobotic surgery. Surg Laparosc Endosc Percutan Tech 2002; 12: 1-5.
13. Schuchert MJ, Pettiford BL, Pennathur A, *et al*. Anatomic segmentectomy for stage I non-small-cell lung cancer: comparison of video-assisted thoracic surgery versus open approach. J Thorac Cardiovasc Surg 2009; 138: 1318-25, e1311.
14. Gharagozloo F, Margolis M, Tempesta B, *et al*. Robot-assisted lobectomy for early-stage lung cancer: report of 100 consecutive cases. Ann Thorac Surg 2009; 88: 380-4.
15. Park BJ, Flores RM: Cost comparison of robotic, video-assisted thoracic surgery and thoracotomy approaches to pulmonary lobectomy. Thorac Surg Clin 2008; 18: 297-300, vii.

機器手臂輔助之胸腔手術－臺大醫院的初步經驗

郭順文　黃培銘　徐紹勛　陳晉興　李章銘

前言：在單一醫學機構進行前瞻性研究，以評估達文西機器手臂輔助之胸腔手術的有效可行性。

方法：在臺大醫院胸腔外科，從 2012 年 2 月至 2012 年 7 月的半年期間，利用達文西機器手臂輔助進行胸腔手術，並記錄相關資料進行分析研究。一共完成了一例胸腺瘤切除、10 例肺葉切除、一例食道切除重建、一例食道良性腫瘤切除。

結果：機器手臂接合時間（docking time）之中位數為 10.5 分鐘（範圍 4-21 分鐘），機器手臂操作時間（console time）之中位數為 183 分鐘（範圍 72-327 分鐘）。沒有病患需要轉換成傳統之胸腔鏡或腹腔鏡進行手術，但有一位病患需要轉換成開胸手術來完成出血的控制。術後併發症包括一例延長之肺部漏氣、一例心律不整 一例肌無力症的暫時性惡化;但沒有任何死亡病例發生。胸管留置天數之中位數為 3 天（範圍 2-11 天），住院天數之中位數為 6 天（範圍 4-19 天）。

結論：在我們的初步經驗中，證實機器手臂輔助之胸腔手術是安全可行的。至於它是否有優於傳統開胸或胸腔鏡手術，仍需更長時間追蹤之前瞻性研究來證實。*(胸腔醫學 **2014; 29: 63-69**)*

關鍵詞：胸腔手術，機器手臂輔助之手術

臺大醫院　外科部
索取抽印本請聯絡：李章銘醫師，臺大醫院　胸腔外科，台北市中山南路 7 號

Laryngeal Small Cell Carcinoma – A Case Presentation and Review of the Literature

Chao-Neng Yang*, Shinn-Liang Lai*, Fang-Chi Lin*,**, Shi-Chuan Chang*,***

Extrapulmonary small cell carcinoma is a rare disease entity that can be found anywhere in the body, especially in the gastrointestinal tract, genitourinary tract, and head and neck areas. Laryngeal small cell carcinoma has a poor prognosis with 2- and 5-year survival rates of only 16% and 5%, respectively. It often presents with local invasiveness to cervical lymph nodes and early distant metastasis. Surgery alone is not enough for tumor eradication, and platinum-based chemotherapy with or without radiotherapy should be considered first. The patient's quality of life should be emphasized because of the poor prognosis. Herein, we report a case of laryngeal small cell carcinoma diagnosed after emergent tracheostomy with the initial presentation of progressive dyspnea followed by desaturation and stridor for 6 months. ***(Thorac Med 2014; 29: 70-76)***

Key words: extrapulmonary small cell carcinoma, laryngeal small cell carcinoma

Introduction

Extrapulmonary small cell carcinoma (EPSCC) is a very rare disease and comprises 2-5% of all small cell carcinoma (SCC). In a review of a cancer database in England for the years 1970-2004, 1618 cases of EPSCC were found. The most common sites of EPSCC were the gastrointestinal (GI) tract (33%), genitourinary (GU) tract (20%), head and neck (11%) and breast (10%) [1]. The larynx is also a common extrapulmonary site of SCC. The epidemiology and risk factors for laryngeal SCC (LSCC) are similar to those of other laryngeal tumors, such as squamous cell carcinoma. Most patients are diagnosed between 60 and 80 years of age, with a slight male predominance; rarely are cases seen before the age of 40 [2]. The prognosis of LSCC is poor, and multi-disciplinary treatment modalities including platinum-based chemotherapy with or without radiotherapy are often required; surgery may be indicated in selected cases. Herein, we report a case of LSCC diagnosed after emergent tracheostomy, with the initial presentation of progressive dyspnea followed by desaturation and stridor for 6 months.

*Department of Chest Medicine, Taipei Veterans General Hospital, Taipei, Taiwan; **School of Medicine, National Yang-Ming University, Taipei, Taiwan; ***Institute of Emergency and Critical Care Medicine, National Yang-Ming University, Taipei, Taiwan
Address reprint requests to: Dr. Shi-Chuan Chang, Department of Chest Medicine, Taipei Veterans General Hospital, No. 201, Section 2, Shih-Pai Road, Taipei 112, Taiwan

Case Presentation

A 79-year-old man, a current smoker with a smoking index of 2 packs per day for 60 years, presented to the emergency department (ER) with a 6-month history of progressive dyspnea, which had worsened in the most recent 2 months, followed by hoarseness and mild dysphagia. Stridor and desaturation were noted when the patient arrived at the ER. Physical examination at the ER showed no palpable mass on the neck. The results of laboratory tests including blood biochemistry and complete blood count were unremarkable. The chest plain film showed increased infiltrates in the bilateral lower lungs only (Figure 1A). Computed tomography (CT) of the thorax disclosed no definite mediastinal or lung parenchymal lesions or evidence of pulmonary embolism, except for a soft tissue lesion in the upper trachea causing airway compromise (Figure 1B). Emergency tracheostomy was performed to establish a patent upper airway. CT scans of the neck revealed asymmetric enlargement of the right vocal cord and infra-hyoid musculature without definite lymphadenopathy, highly suggestive of laryngeal cancer. (Figure 2; white arrow) Subcutaneous emphysema was noted after the emergency tracheostomy (Figure 2; white arrow head), but it later subsided spontaneously. On laryngoscopic examination, a tumor growth was noted involving bilateral sub-glottic and right glottic areas (Figure 3A & 3B). The histopathologic examination of the tumor biopsy showed tumor cells infiltrating the mucosa and submucosal tissues with focal necrosis and a crushing effect (Figure 4A & 4B). The cells were positive for cytokeratin (AE1/AE3), synaptophysin, chromogranin and CD56, but negative for LCA (Figure 5); the picture was compatible with SCC. The whole body bone scans and brain MRI revealed no distant metastasis. By definition, the clinical staging was cT3N0M0, stage III. Local radiotherapy with a suboptimal dose of 17.5 Gy in

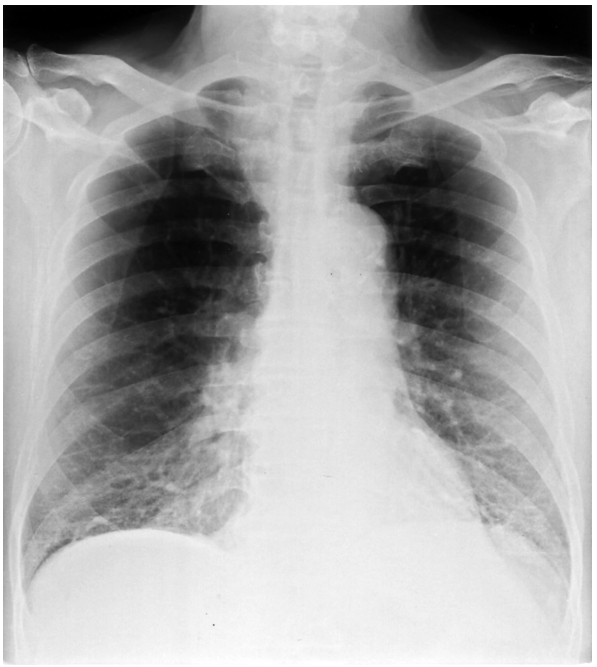

Fig. 1A. Chest plain film reveals increased infiltrates in bilateral lower lungs.

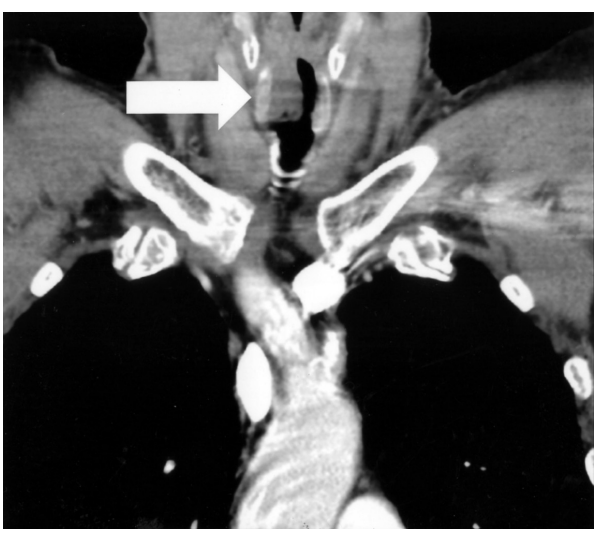

Fig. 1B. CT scans of the thorax reveal a soft tissue lesion in the upper trachea. (arrow)

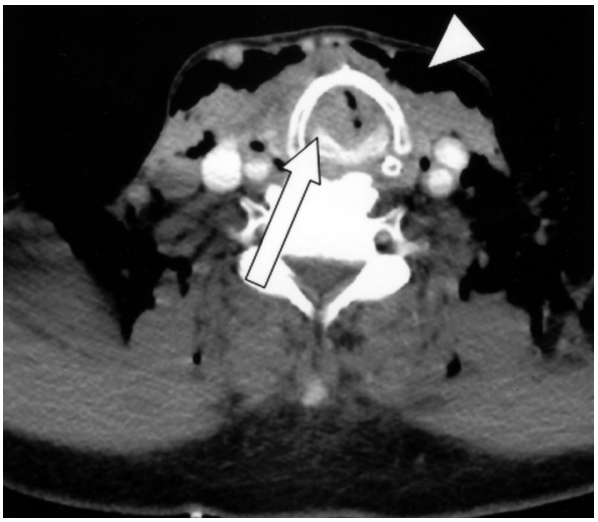

Fig. 2. Neck CT scans demonstrate asymmetric enlargement of the right vocal cord and infra-hyoid musculature (white arrow), and subcutaneous emphysema. (white arrow head)

7 fractions was started 3 weeks after diagnosis, due to intolerance of radiotherapy, followed by 2 cycles of systemic chemotherapy with etoposide and cisplatin (45 mg/m^2, respectively). However, the patient had recurrent pneumonia beginning 2 weeks after the second course of chemotherapy and expired 4 months after the diagnosis of LSCC, due to septic shock.

Discussion

EPSCC is a rare disease and could arise anywhere in the body. The 3 most common sites of EPSCC are the GI tract, GU tract and head and neck regions. The initial manifestations depend on the site of involvement, but may include para-neoplastic syndromes. EPSCC usually presents with widespread and early metastases. Although some patients with locoregional disease may be treated successfully with aggressive therapy, most patients relapse and the overall prognosis is poor, with a 5-year survival rate of around 15% [3]. The median survival for

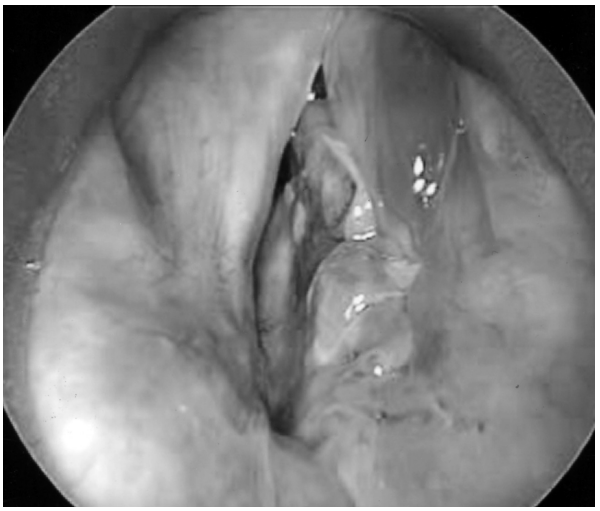

(A)

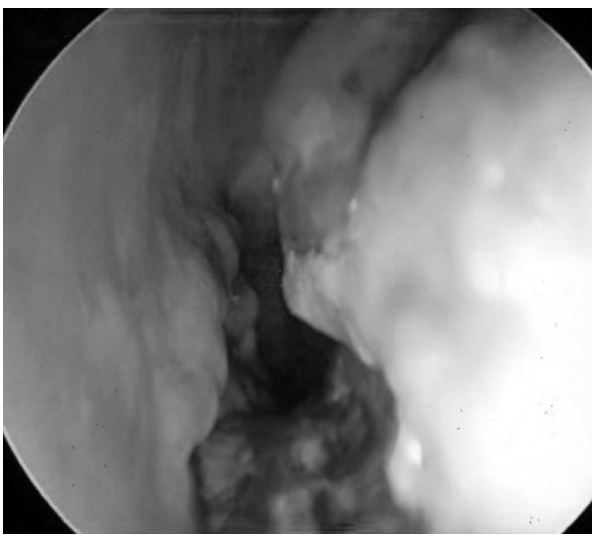

(B)

Fig. 3A & 3B. Laryngoscopic findings include a tumor growth involving the right glottic (A) and bilateral sub-glottic areas. (B)

limited and extensive disease ranged from 1.4 to 3.5 years and 8 to 12 months, respectively [4-5]. EPSCC of the breast had a better prognosis than EPSCC in other sites [1]. The larynx is the most common site of EPSCC in head and neck areas. Endocrine neoplasms of the larynx are composed of an epithelial (carcinoma) type and a neural (paraganglioma) type. LSCC is an

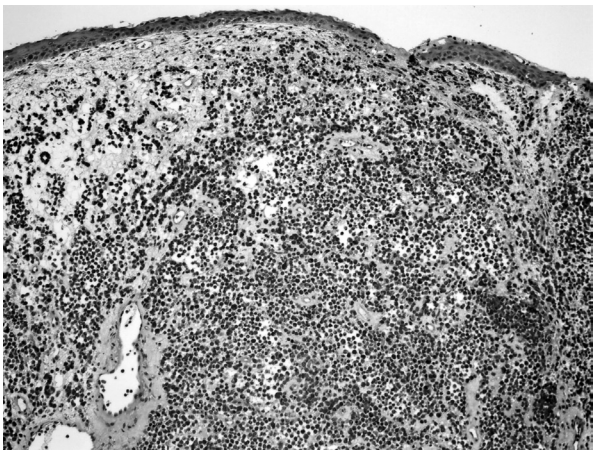

Fig. 4A. Photomicrograph showing laryngeal mucosal tissue with infiltrative tumor cells in sub-epithelial stromal tissue. (H&E; x 200)

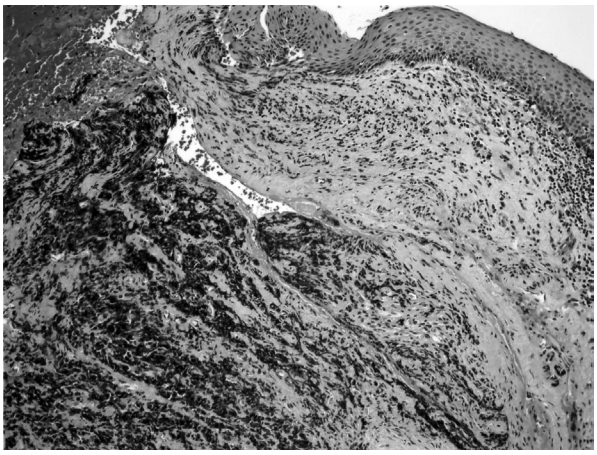

Fig. 4B. Histopathological examination shows the presence of a crush artifact. (H&E; x 200)

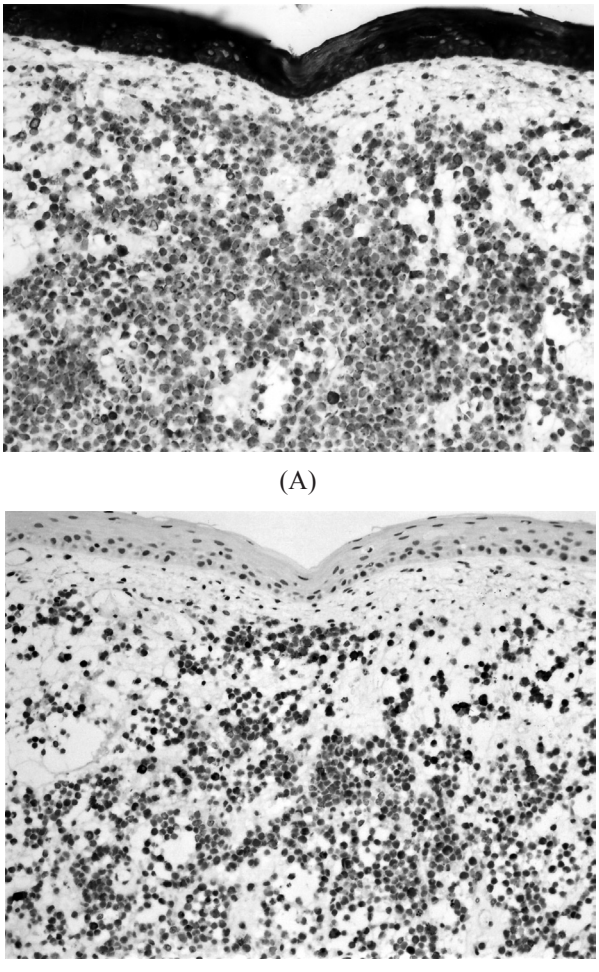

Fig. 5. Immunochemical stains of cytokeratin AE1/AE3 (A), synaptophysin (B), chromogranin-A (C) and CD56 (D) show positive staining.

epithelial type and has a poorer prognosis than typical carcinoid or atypical carcinoid tumors. LSCC can co-exist with other tumor types such as adenocarcinoma or squamous cell carcinoma [6]. Cervical lymph node metastases are often the initial mode of tumor spread, followed by distant metastases which result in a poor prognosis [7].

Unlike typical or atypical carcinoid tumors, surgical intervention is not initially considered in cases of LSCC. Before treatment, patients should be evaluated to exclude a primary lung SCC or evidence of distant metastases. LSCC is staged according to the TNM staging system, as is squamous cell carcinoma of the larynx [8]. The estimated 2- and 5-year survival rates of LSCC are 16% and 5%, respectively. In a review, about 70% of patients with LSCC died of disease with widespread metastases, with a mean survival time of 9.8 months (range, 1-26 months) [9]. Primary chemo-radiotherapy is the treatment of choice, with surgery taking a secondary role given the extremely high rate of distant metastasis [10]. The chemotherapy is the same as that used for extensive SCC of the lung, and platinum-based chemotherapy should be considered. Systemic chemotherapy combined with radiotherapy has been suggested as a primary treatment modality for LSCC because of the improved survival of the patients [11]. However, the goal of treatment for LSCC should be quality of life for the patients because of the poor prognosis.

Conclusion

LSCC is the most lethal neuroendocrine neoplasm of the larynx, with 2- and 5-year survival rates of only 16% and 5%, respectively. Cervical lymph node metastasis and early distant metastasis are common, which often make surgical resection less likely. Platinum-based chemotherapy with or without radiotherapy is suggested as a current treatment modality. Surgical intervention is usually reserved because of the aggressive clinical course. Even so, the prognosis is very poor.

References

1. Wong YN, Jack RH, Mak V, *et al*. The epidemiology and survival of extrapulmonary small cell carcinoma in South East England, 1970-2004. BMC Cancer 2009; 9: 209.
2. Ferlito A. Diagnosis and treatment of small cell carcinoma of the larynx: a critical review. Ann Otol Rhinol Laryngol 1986; 95: 590-600.
3. Walenkamp AM, Sonke GS, Sleijfer DT, *et al*. Clinical and therapeutic aspects of extrapulmonary small cell carcinoma. Cancer Treat Rev 2009; 35: 228-36.
4. Brennan SM, Gregory DL, Stillie A, *et al*. Should extrapulmonary small cell cancer be managed like small cell lung cancer? Cancer 2010; 116: 888-95.
5. Ochsenreither S, Marnitz-Schultze S, Schneider A, *et al*. Extrapulmonary small cell carcinoma (EPSCC): 10 years' multi-disciplinary experience at Charité. Anticancer Res 2009; 29: 3411-5.
6. Jaiswal VR, Hoang MP, Primary combined squamous and small cell carcinoma of the larynx: a case report and review of the literature. Arch Pathol Lab Med. 2004 Nov; 128(11): 1279-82.
7. Mills SE, Cooper PH, Garland TA, *et al*. Small cell undifferentiated carcinoma of the larynx. Report of two patients and review of 13 additional cases. Cancer 1983; 51: 116-20.
8. Edge SB, Byrd DR, Compton CC, *et al*. American Joint Committee on Cancer Staging Manual, Springer, New York 2009. 57.
9. Gnepp DR, Ferlito A, Hyams V, *et al*. Primary anaplastic small cell (oat cell) carcinoma of the larynx. Review of the literature and report of 18 cases. Cancer 1983; 51: 1731-45.
10. Ferlito A, Silver CE, Bradford CR, *et al*. Neuroendocrine neoplasms of the larynx: an overview. Head Neck 2009; 31: 1634-46.

11. Monroe AT, Morris CG, Lee E, *et al*. Small cell carcinoma of the head and neck: The University of Florida experience. J Hong Kong College of Radiologists, 2005, vol. 8, no. 2, 83-86.

咽喉小細胞癌：個案報告與文獻探討

楊朝能 * 賴信良 * 林芳綺 *,** 張西川 *,***

肺外小細胞癌症是一個相當罕見的疾病，身體任何地方都可能產生。根據文獻報告記載，其最常出現於腸胃道、生殖泌尿道以及頭頸部。頭頸部小細胞癌中以咽喉小細胞癌最為常見，但其預後相當差，兩年以及五年的存活率分別約為 16% 以及 5%。預後較差的主要原因是因其常有頸部淋巴結侵犯以及早期遠處轉移。目前，單以手術治療咽喉小細胞癌是不夠的，首選治療應以白金為基礎的化學治療輔以或不輔以放射線治療。即便如此，咽喉小細胞癌的預後仍相當差，所以在考慮治療方式時應該以患者的生活品質為優先考量。在此我們提出一位經緊急氣切手術後才診斷的咽喉小細胞癌案例，其臨床則是以六個月內漸進式呼吸困難、喘鳴以及血氧低下來表現。*(胸腔醫學* ***2014; 29: 70-76)***

關鍵詞：肺外小細胞癌症，咽喉小細胞癌

* 台北榮民總醫院　胸腔部，** 國立陽明大學醫學院，*** 國立陽明大學　重症醫學研究所
索取抽印本請聯絡：張西川醫師，台北榮民總醫院　胸腔部，台北市 112 北投區石牌路二段 201 號

Sarcoidosis Presenting with Concurrent Pericardial and Pleural Effusion – A Case Report

Jung-Te Chiu*, Jeng-Yuan Hsu*,**, Kun-Chieh Chen*

Sarcoidosis is a granulomatous disorder with multisystem involvement, including the lungs (90%), skin, eyes, lymph nodes, spleen, liver, heart, central nervous system, and kidneys, and with a predilection for adults younger than 40 years. Sarcoidosis affects females more than males. Diagnosis of sarcoidosis is made by clinico-radiologic and histopathologic findings of non-caseating granuloma, as well as exclusion of other granulomatous diseases, such as tuberculosis, fungus, and malignancy. However, the incidence of sarcoidosis with concurrent pericardial and pleural effusion is extremely low. Herein, we present the case of a 57-year-old female patient with concomitant pericardial and pleural effusion with a good response to prednisolone for 4 months. ***(Thorac Med 2014; 29: 77-84)***

Key words: sarcoidosis, pleural effusion, pericardial effusion

Introduction

Sarcoidosis is a granulomatous disorder characterized by multisystem involvement, including the lungs (90%), skin, eyes, lymph nodes, spleen, liver, heart, central nervous system, and kidneys [1]. The disease shows a predilection for adults less than 40 years of age, peaking in those aged 20-29 years [2]; 30-60% of sarcoidosis patients are asymptomatic, with 85-95% having abnormal findings on chest radiography [1]. Bilateral hilar lymphadenopathy is the most common chest radiographic feature of sarcoidosis [3]. The chest radiographic Scadding staging system [4] was developed to define the 4 stages of sarcoidosis, as follows: stage 0 (normal); stage I (bilateral hilar lymphadenopathy without pulmonary infiltrates); stage II (bilateral hilar lymphadenopathy plus pulmonary infiltrates); stage III (parenchymal infiltrates without bilateral hilar lymphadenopathy); stage IV (extensive lung fibrosis). High-resolution computed tomography (HRCT) chest scans are better than chest radiography at illustrating lung parenchymal details and mediastinal and hilar structures, and distinguishing lung inflammation from fibrosis [5]. Characteristic features of sarcoidosis on CT include mediastinal and/or bilateral hilar lymphadenopathy, micronodules along bronchovascular bundles, a predilection

*Division of Chest Medicine, Department of Internal Medicine, Taichung Veterans General Hospital, Taichung, Taiwan; **Division of Critical Care & Respiratory Therapy, Department of Internal Medicine, Taichung Veterans General Hospital, Taichung, Taiwan
Address reprint requests to: Dr. Kun-Chieh Chen, Division of Chest Medicine, Department of Internal Medicine, Taichung Veterans General Hospital, 1650 Taiwan Boulevard Sect. 4, Taichung, Taiwan 40705, Taiwan

for middle and upper lung zones, an axial distribution, pleural or subpleural nodules, septal and nonseptal lines, confluent nodular opacities with consolidation and ground-glass opacities [6]. The diagnosis of sarcoidosis is based on the clinico-radiologic features, supported by histopathologic evidence demonstrating non-caseating granuloma and exclusion of other granulomatous diseases [7].

Postmortem studies indicated myocardial involvement in about 25% of sarcoidosis patients with clinical manifestations of arrhythmias, conduction disturbances, or cardiomyopathy [8]; 21% (17 of 81) of sarcoidosis patients had a mild to moderate amount of pericardial effusion on echocardiography [9]. Pleural involvement in sarcoidosisis is a rare manifestation [10].

Sarcoidosis presenting with pleural and pericardial effusion is extremely rare. We present herein the case of a female patient with sarcoidosis with concomitant pericardial and pleural effusion.

Case Report

A 57-year-old non-smoking female presented with chronic productive cough for 1 year. She had chest tightness and dyspnea on exertion, along with body weight loss of 10 kg in 1 year. She visited our chest medicine OPD, where the physical examination was unremarkable. Nevertheless, the chest radiograph (Figure 1) revealed bilateral hilar lymph nodes enlargement with bilateral pleural effusion. Pulmonary function tests revealed FEV_1 of 0.89 liter (36% of predicted), FVC of 1.8 liter (60% of predicted), FEV_1/FVC at 50%, a negative bronchodilator test, TLC 110% of predicted, and DLCO 81% of predicted. EKG revealed a first-degree atrioventricular block without significant ST-T change. Echocardiography showed normal left ventricular wall motion and ejection fraction without significant valvular dysfunction. However, a small amount of pericardial effusion was noted. Contrast-enhanced chest CT (Figures 2a, 2b, 2c, 2d) revealed multiple mediastinal and

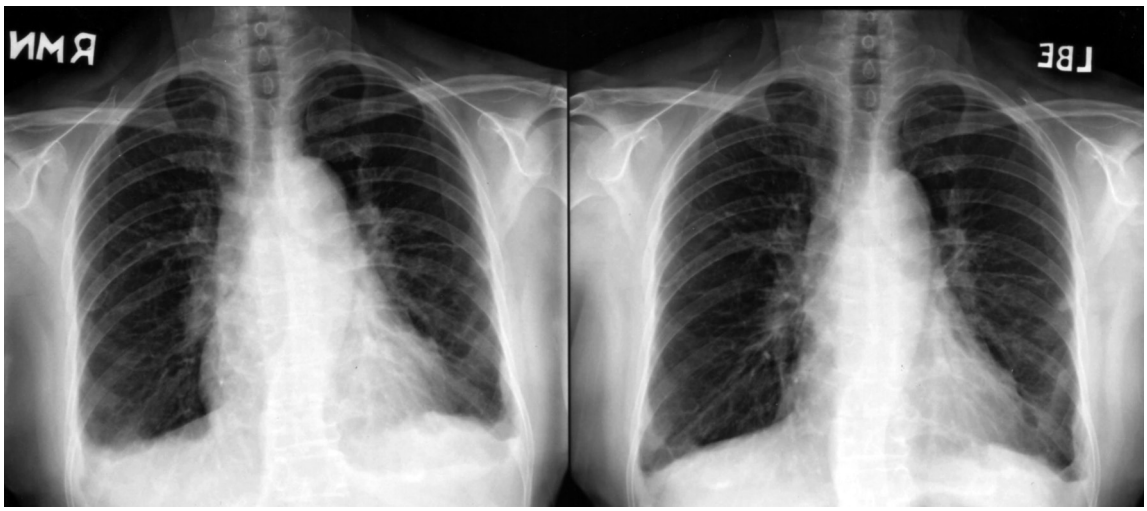

(a) (b)

Fig. 1. Baseline and post-treatment CXR. (1a) Chest radiography showed bilateral hilar lymph node enlargement, mediastinal lymphadenopathy, and bilateral pleural effusion. (1b) Follow-up chest radiography showed diminished bilateral pleural effusion

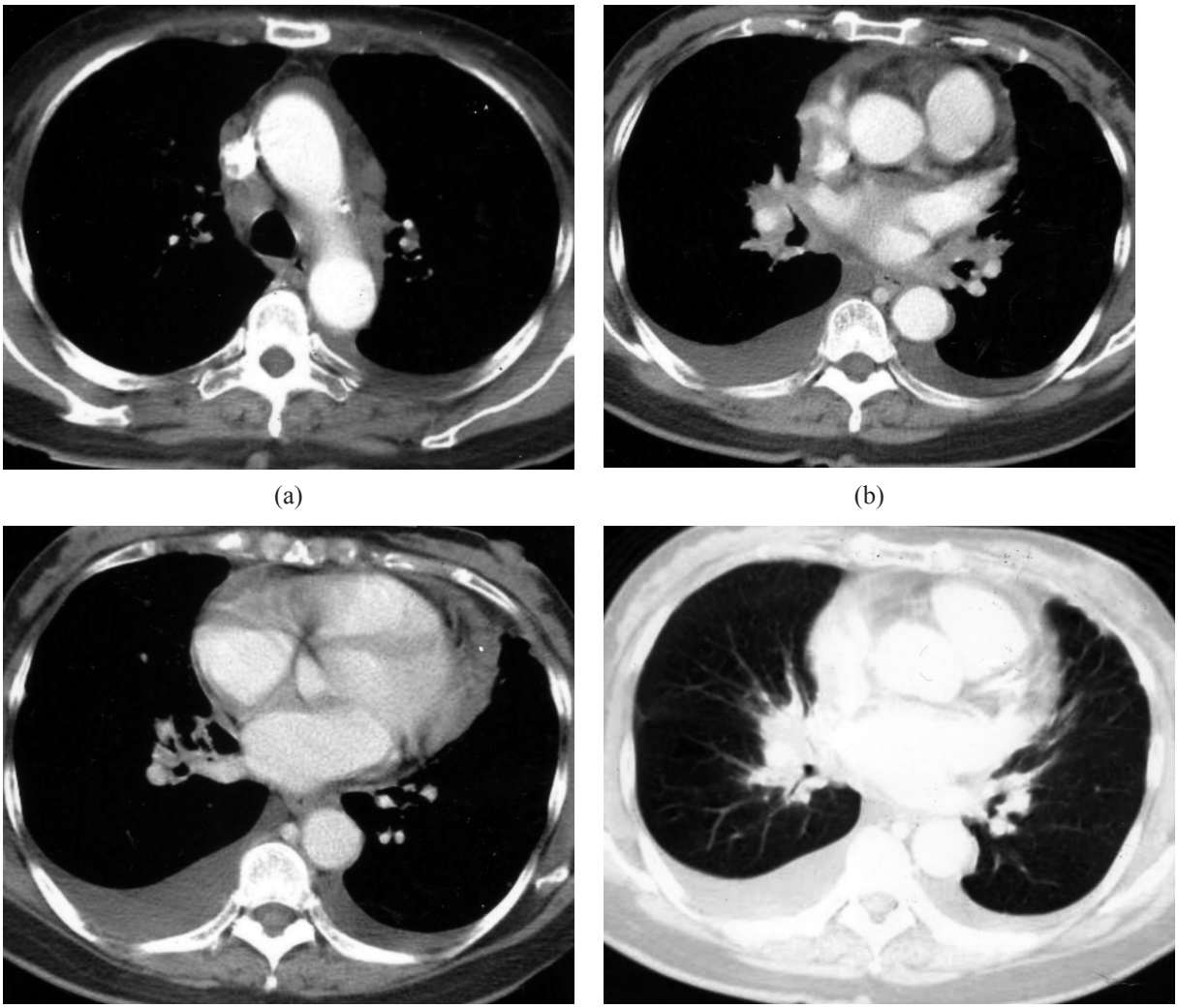

(a) (b)

(c) (d)

Fig. 2. Contrast-enhanced chest CT of the present case. (2a) Chest CT showed mediastinal lymphadenopathy. (2b) Chest CT showed bilateral hilar lymphadenopathy and bilateral pleural effusion with pleural plaque. (2c) Chest CT showed pericardial effusion and bilateral pleural effusion. (2d) Chest CT (lung window) showed bilateral peribronchovascular thickening

bilateral hilar lymphadenopathies with peribronchovascular thickening. CT also revealed irregular thickening of the pericardium with a small amount of pericardial effusion and multiple pleural nodularity with a bilateral small amount of pleural effusion. Neither pericardiocentesis nor thoracocentesis could be performed due to the small amount of fluid. Thus, we performed bronchoscopy (Figures 3a, 3b, 3c), which revealed multiple endobronchial "cobblestone-like" nodules along the bronchial trees. Endobronchial nodule biopsy (Figures 4a, 4b) revealed non-caseating granulomatous inflammation. Acid-fast stain, mycobacterial culture, fungus culture and bacterial culture all yielded negative findings. She was diagnosed as having sarcoidosis based on the chest radiograph, chest CT and histopathologic report findings, and by excluding malignancy, fungus and tuberculosis. Her symptoms of chronic cough and

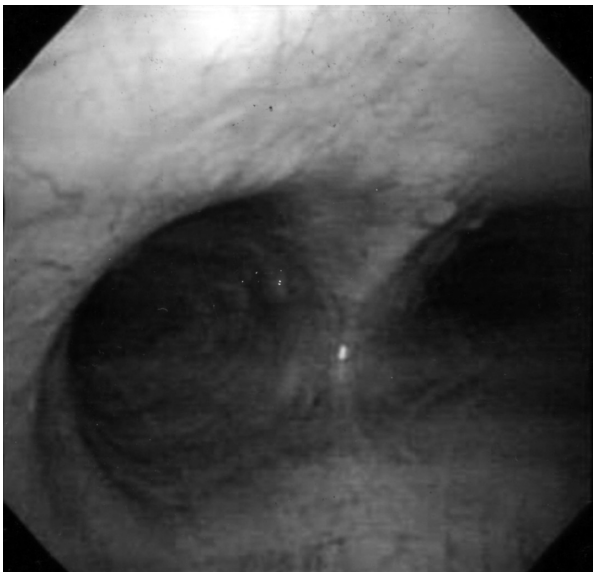

(a)

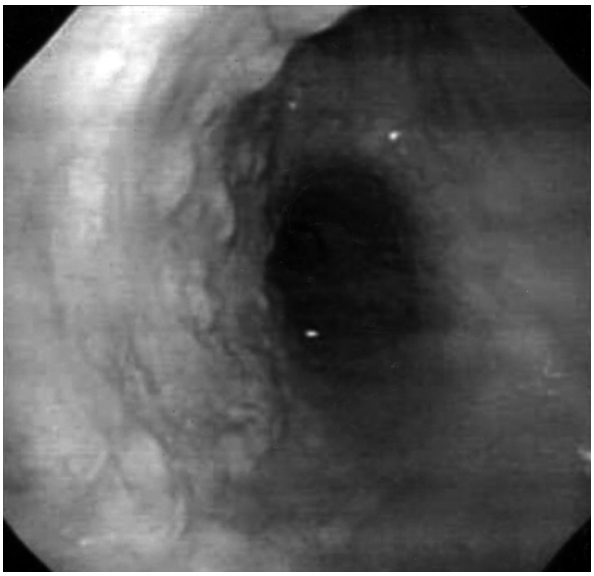

(b)

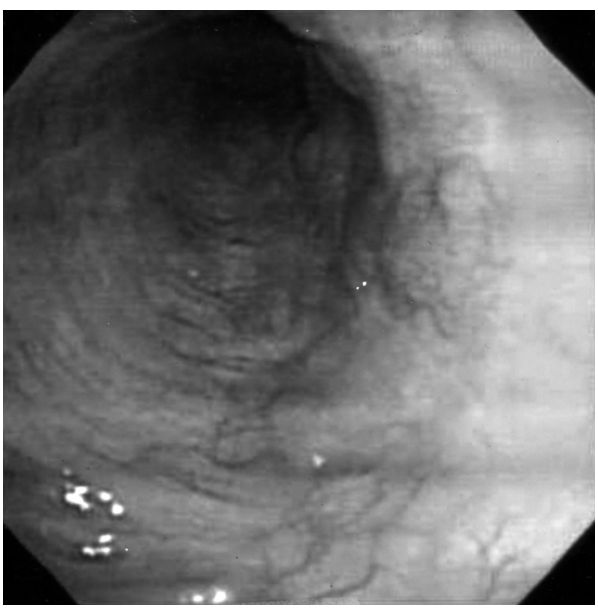

(c)

Fig. 3. Bronchoscope picture. (3a) Bronchoscope showed multiple cobblestone-like nodules at the carina, along the bilateral main bronchus. (3b) Bronchoscope showed multiple cobblestone-like nodules at the right main bronchus. (3c) Bronchoscope showed multiple cobblestone-like nodules at the left main bronchus

dyspnea were relieved with oral predinisolone 10 mg BID for 4 months. The follow-up chest radiograph (Figure 1b) and contrast-enhanced chest CT (Figures 5a, 5b, 5c) both revealed improvement of the mediastinal and bilateral hilar lymphadenopathy and decreased pericardial and pleural effusion.

Discussion

Pleural involvement is a rare manifestation of sarcoidosis. In a study of 181 patients with biopsy-proven sarcoidosis, only 2.8% (5 of 181) revealed pleural effusion on ultrasound [11]. Sarcoidosis was established as the cause of pleural effusion in only 1.1% (2 of 181) of

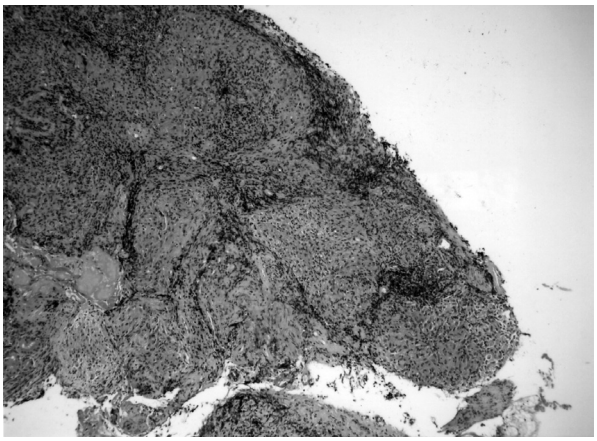

(a)

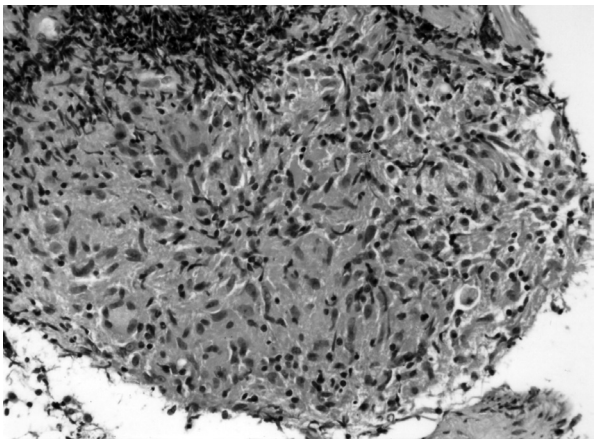

(b)

Fig. 4. Histopathology report. (4a) Bronchoscopic biopsy showed multiple non-caseating granulomas (H&E stain 100X). (4b) Bronchoscopic biopsy showed non-caseating granuloma composed of epithelioid cells (H&E stain 400X).

these patients (1 patient had bilateral pleural effusion with pleura biopsy-confirmed sarcoidosis, and 1 was clinically diagnosed as having pleural sarcoidosis based on clinico-radiologic findings). Two of the other 3 patients with pleural effusion were clinically diagnosed as having congestive heart failure-related pleural effusion and the third had parapneumonic pleural effusion.

Most instances of pleural effusion in the course of sarcoidosis involve a small to moderate amount, and are more commonly seen on the right side (45%) than the left (33%), for an unknown reason. Bilateral pleural effusion was reported in 22% of cases [11]. Moreover, sarcoidosis-related pleural effusion was seen in 1 of 9 patients (11.1%) who had an exacerbation of pulmonary sarcoidosis, compared to 1 of 172 patients (0.5%) who did not have an exacerbation ($p < 0.4$), which suggested that sarcoidosis with pleural effusion may have a substantial tendency to exacerbation. Pleural effusion in the course of sarcoidosis is most commonly an exudate and lymphocyte-predominant [11]. A definite diagnosis of pleural sarcoidosis should be based on a histopathological examination, after ruling out all other causes of pleural effusion, such as tuberculosis, malignancy or congestive heart failure [12].

In the majority of cases, the effusion resolves spontaneously within 1 to 3 months [10]. Systemic corticosteroids may be used only in symptomatic patients and patients with recurrent pleural effusion, which may lead to chronic pleural irritation and thickening, resulting in fibrothorax.

Cardiac manifestations include bundle branch block, arrhythmia, congestive heart failure, pericarditis, and cardiomyopathy. Asymptomatic minimal pericardial effusion has been shown to occur in 20% of cases [9]. Endomyocardial biopsy showing non-caseating granulomas confirms the diagnosis of cardiac sarcoidosis, but the diagnostic yield from the procedure is low. Thus, sarcoid-like patients with cardiac dysfunction, ECG abnormalities, or thallium-201 imaging defects should be presumed to have cardiac sarcoidosis [9]. Shiff and associates reported the first proved case of clinically significant pericardial lesion due to sarcoid granulomas in the pericardium [13].

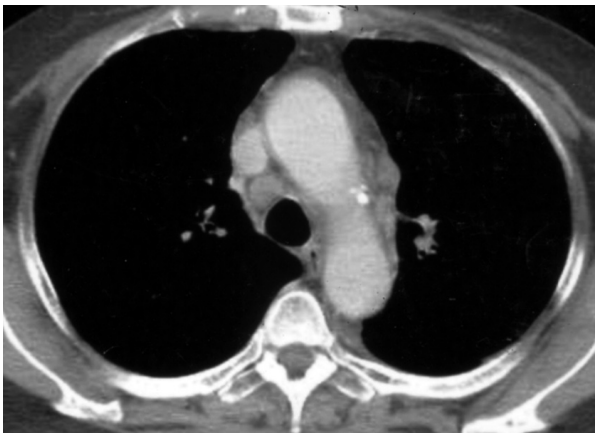

(a)

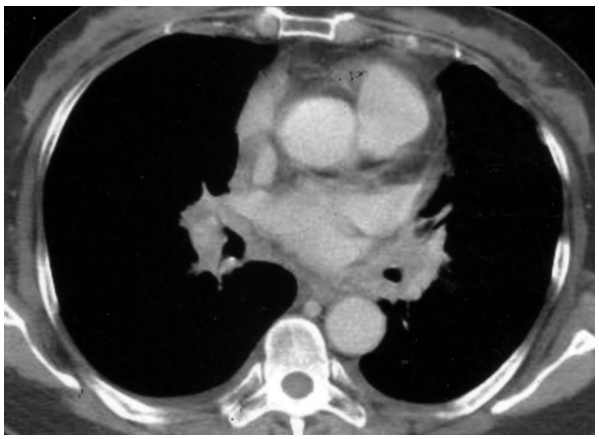

(b)

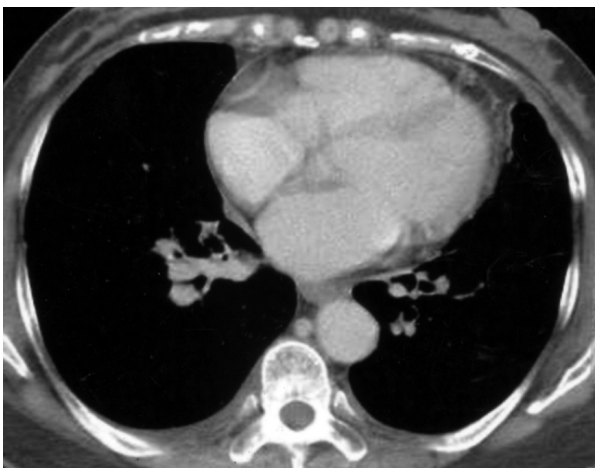

(c)

Fig. 5. Follow-up chest CT. (5a) Chest CT showed shrunken mediastinal lymphadenopathy. (5b) Chest CT showed diminished bilateral pleural effusion and shrunken bilateral hilar lymphadenopathy. (5c) Chest CT showed diminished pericardial effusion

Patients with concurrent pleural and pericardial effusions need to be investigated for rheumatological diseases, occult malignancies, and chronic infections such as HIV, tuberculosis, hepatitis, and syphilis [14].

The bronchoscope biopsy of our patient revealed non-caseating granuloma with negative findings for malignancy, fungus, and tuberculosis. We could not perform pericardial and pleural biopsy to confirm the definitive diagnosis of pericardial and pleural sarcoidosis. However, echocardiography revealed normal left ventricular wall motion and systolic ejection fraction; other common causes of bilateral pleural effusion such as hyper/hypothyroidism, collagen vascular disease, and cirrhosis were excluded. The patient's clinical status improved and follow-up chest CT revealed decreased pericardial and pleural effusion with oral prednisolone 20 mg treatment only, which is indicative of sarcoidosis with pleural and pericardial involvement that responded to steroid.

In conclusion, sarcoidosis presenting with pleural and pericardial effusion is extremely rare. Pleural effusion in the course of sarcoidosis is most commonly seen on the right side, and bilateral pleural effusion is reported in 22% of patients. The pleural effusion in the course of sarcoidosis is most commonly an exudate and lymphocyte-predominant. Systemic corticosteroids alone may be used in symptomatic patients and patients with recurrent pleural and pericardial effusion.

References

1. Lynch JP, 3rd, Ma YL, Koss MN, *et al*. Pulmonary sarcoidosis. Semin Respir Crit Care Med 2007; 28: 53-74.
2. Gordis, L. 1973. Sarcoidosis: Epidemiology of Chronic Lung Diseases in Children.The John Hopkins University

Press, Baltimore. 53-78.
3. Lynch JP, 3rd, Kazerooni EA, Gay SE. Pulmonary sarcoidosis. Clin Chest Med 1997; 18: 755-85.
4. Scadding JG. Prognosis of intrathoracic sarcoidosis in England. A review of 136 cases after five years' observation. Br Med J 1961; 2: 1165-72.
5. Bergin CJ, Bell DY, Coblentz CL, *et al*. Sarcoidosis: correlation of pulmonary parenchymal pattern at CT with results of pulmonary function tests. Radiology 1989; 171: 619-24.
6. Lynch JP, 3rd. Computed tomographic scanning in sarcoidosis. Semin Respir Crit Care Med 2003; 24: 393-418.
7. Statement on sarcoidosis. Joint Statement of the American Thoracic Society (ATS), the European Respiratory Society (ERS) and the World Association of Sarcoidosis and Other Granulomatous Disorders (WASOG) adopted by the ATS Board of Directors and by the ERS Executive Committee, February 1999. Am J Respir Crit Care Med 1999; 160: 736-55.
8. Silverman KJ, Hutchins GM, Bulkley BH. Cardiac sarcoid: a clinicopathologic study of 84 unselected patients with systemic sarcoidosis. Circulation 1978; 58: 1204-11.
9. Angomachalelis N, Hourzamanis A, Salem N, *et al*. Pericardial effusion concomitant with specific heart muscle disease in systemic sarcoidosis. Postgrad Med J 1994; 70 (Suppl 1): S8-12.
10. Soskel NT, Sharma OP. Pleural involvement in sarcoidosis. Curr Opin Pulm Med 2000; 6: 455-68.
11. Huggins JT, Doelken P, Sahn SA, *et al*. Pleural effusions in a series of 181 outpatients with sarcoidosis. Chest 2006; 129: 1599-604.
12. Cohen M, Sahn SA. Resolution of pleural effusions. Chest 2001; 119: 1547-62.
13. Shiff AD, Blatt CJ, Colp C. Recurrent pericardial effusion secondary to sarcoidosis of the pericardium. N Engl J Med 1969; 281: 141-3.
14. Kim JS, Judson MA, Donnino R, *et al*. Cardiac sarcoidosis. Am Heart J 2009; 157: 9-21.

類肉瘤同時合併心包膜及肋膜積水－病歷報告

邱榮德 * 許正園 *,** 陳焜結 *

類肉瘤為影響多重系統的結節性疾病，包含肺部（90%）、皮膚、眼睛、淋巴結、脾臟、肝臟、心臟、中樞神經系統、腎臟…等。類肉瘤好發於 40 歲以下成人，且好犯女性。類肉瘤的診斷建立於臨床症狀與影像學，配合病理切片診斷，最重要的是要排除其他疾病，如結核、黴菌、惡性腫瘤…等。然而，類肉瘤合併心包膜及肋膜積水的案例非常少見。我們報告一位 57 歲女性病人，診斷為類肉瘤合併心包膜及肋膜積水，且經有四個月的類固醇治療後有顯著的反應。*(胸腔醫學* ***2014; 29: 77-84)***

關鍵詞：類肉瘤，心包膜積水，肋膜積水

台中榮民總醫院　內科部　胸腔內科 *，台中榮民總醫院　內科部　呼吸治療科 **
索取抽印本請聯絡：陳焜結醫師，台中榮民總醫院　內科部　胸腔內科，台中市台灣大道四段 1650 號

Human Pulmonary Dirofilariasis Coexisting with Lung Cancer

Yi-Han Hsiao, Jia-Yih Feng, Yu-Chung Wu*, Yi-Chen Yeh**,
Yu-Chin Lee, Chao-Hua Chiu

Dirofilariasis is a common parasite infection in stray dogs caused by *Dirofilaria immitis* (dog heartworm). Under very rare circumstances, it can cause human pulmonary lesion via a vector/intermediate host, the mosquito. It typically presents as a well-circumscribed, peripheral, solitary pulmonary nodule on radiograph, and is easily confused with lung malignancy. Diagnosis rests on histopathologic identification of the excised worm. We reported a 48-year-old female with a rare coexistence of pulmonary dirofilariasis and lung cancer. Clinical suspicion of a mixed etiology should be maintained in a lung cancer patient with a separate lung nodule. An undetermined pulmonary nodule should not preclude the possibility of surgical intervention for lung cancer patients with resectable disease. ***(Thorac Med 2014; 29: 85-91)***

Key words: pulmonary dirofilariasis, lung cancer, solitary pulmonary nodule

Introduction

Dirofilaria immitis (dog heartworm) is a parasitic roundworm that is spread through the bites of mosquitoes. The adult worms reside in the pulmonary artery and right ventricle, and shed microfilariae into the blood stream, causing signs of right ventricular outflow obstruction and congestive heart failure in dogs. The prevalence of adult worms in the stray dog population was 57% in northern Taiwan [1].

Dirofilaria immitis can infect humans under very rare circumstances. In these cases, the human becomes a 'dead end' host. Dirofilariasis may cause pulmonary and cutaneous infection in humans. Cutaneous infection occurs when the larvae die after inoculation into the subcutaneous tissue and cause an urticarial eruption. If a larva reaches the heart, it dies in the right ventricle, embolizes into the pulmonary artery, and becomes organized into a necrotic and fibrotic nodule in the lung periphery [2]. This "coin-like" nodule, as it appears on radiograph, is usually confused with lung malignancy until removed surgically.

Most cases were reported in the southeastern or Gulf states of the United States in patients in their 5th or 6th decade of life, with a male to fe-

Department of Chest Medicine; *Division of Chest Surgery, Department of Surgery; **Department of Pathology and Laboratory Medicine, Taipei Veterans General Hospital, Taipei, Taiwan
Address reprint requests to: Dr. Chao-Hua Chiu, Department of Chest Medicine, Taipei Veterans General Hospital, 201 Shih-Pai Road, Section 2, Taipei 11217, Taiwan

male ratio of 2:1 [3-4], but sporadic cases have been reported all over the world. The first documented infection resulting in pulmonary infarction was described by Dashiell in 1961 [5]. Five cases have been reported in Taiwan to date, the first case by Yang *et al* in 1993 [6]. Herein we report a case of lung adenocarcinoma with a nearby pulmonary nodule that was initially diagnosed as intrapulmonary metastasis (T4 disease), but the final pathology review proved it to be human pulmonary dirofilariasis.

Case Report

A 48-year-old female came to our outpatient clinic due to intermittent cough with scanty sputum for 3 months. She denied other symptoms such as fever, shortness of breath, body weight loss, chest pain, chest tightness, or hemoptysis. The patient had a past history of hypertension and type 2 diabetes mellitus which had been well-controlled medically for years. The latest HbA1C was 6.0%, and a recent home blood pressure reading was around 110/80 mmHg. The physical examination showed no abnormal finding. She was a housewife, and denied cigarette smoking, alcohol consumption, or allergy to food or drugs. There was no travel history in the past 6 months, no contributory family history, and no pet breeding history. The leukocyte count was 6100/cumm with a normal differential, the hemoglobin level was 13.4 g/dl, and the platelet count was 279000/cumm. Liver function and renal function were both within normal limits with values of alanine transaminase and aspartate transaminase of 15 and 19 mg/dl, respectively, and a creatinine level of 0.65 mg/dl. Chest radiography and computed tomography (CT) revealed a 2.1 cm lobulated pulmonary nodule in the right lower lobe (RLL) and a small triangular opacity in the right middle lobe (RML) of the lung (Figure 1). CT-guided biopsy of the RLL nodule was performed and the pathology revealed well-differentiated adenocarcinoma of the lung. Whole body positron emission tomography/computed tomography (PET/CT) showed no abnormal fluorodeoxyglucose (FDG) uptake at both pulmonary nodules, and no distant metastasis. The preoperative pulmonary function test showed restrictive ventilatory impairment with FEV_1 of 0.83L (43% predicted), FVC of 1.13L (47% predicted), TLC of 2.71L (67% predicted) and impaired DL_{CO} (41% predicted). Because of the poor pulmonary reserve, the patient underwent video-assisted thoracic surgery (VATS) with RLL and RML wedge resection instead of lobectomy. The pathology examination of the RML nodule unexpectedly revealed a partial portion of larvae of nematode with a general body cavity, cuticle and sub-cuticle muscular layer in a blood vessel highlighted by elastic-Van Gieson stain, compatible with the diagnosis of pulmonary dirofilariasis (Figure 2).

Discussion

The differential diagnosis of multiple pulmonary nodules on chest radiography includes neoplastic, infectious, inflammatory, vascular, and congenital lesions, which usually can be determined by clinical history. However, further imaging tests and/or biopsy is sometimes required for diagnosis.

Chest CT is most often used to evaluate pulmonary nodules through their size, shape, margin, calcification, and growth rate. For example, large pulmonary nodules with a lobulated margin, thick-walled cavitation, stippled calcification or rapid growth rate are considered

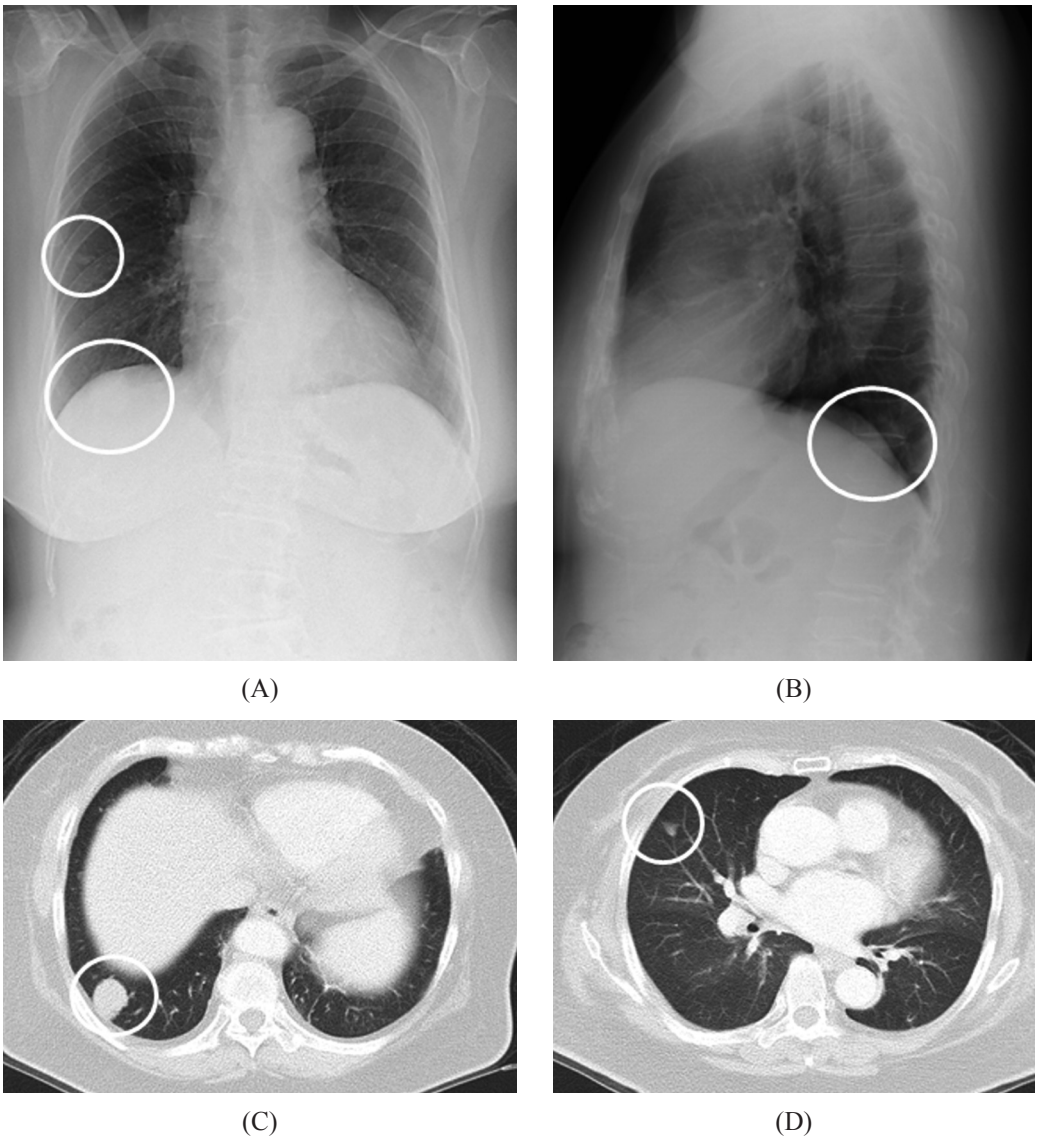

Fig. 1. (A, B) Chest X-ray showed 2 nodular lesions, one each in the right middle lung and right lower lung field, respectively. (C, D) Computed tomography showed a lobulated soft tissue nodule (2.1 cm) in the right lower lobe (C) and a small triangular opacity in the right middle lobe (D).

to have a malignant etiology. In patients with a known malignant primary tumor, multiple pulmonary nodules exceeding 5 mm in diameter are more likely to be malignant than benign [7]. In our case, the lobulated soft tissue nodule in the RLL suggested malignancy, but the nature of the small opacity in the RML was difficult to determine preoperatively.

Integrated PET/CT provides both anatomic and metabolic information and has high sensitivity in distinguishing malignant from benign pulmonary lesions. However, several factors affect the maximum standardized uptake values, causing low metabolic activity and a false-negative result on PET/CT. These factors include the histological type of the tumors (e.g.,

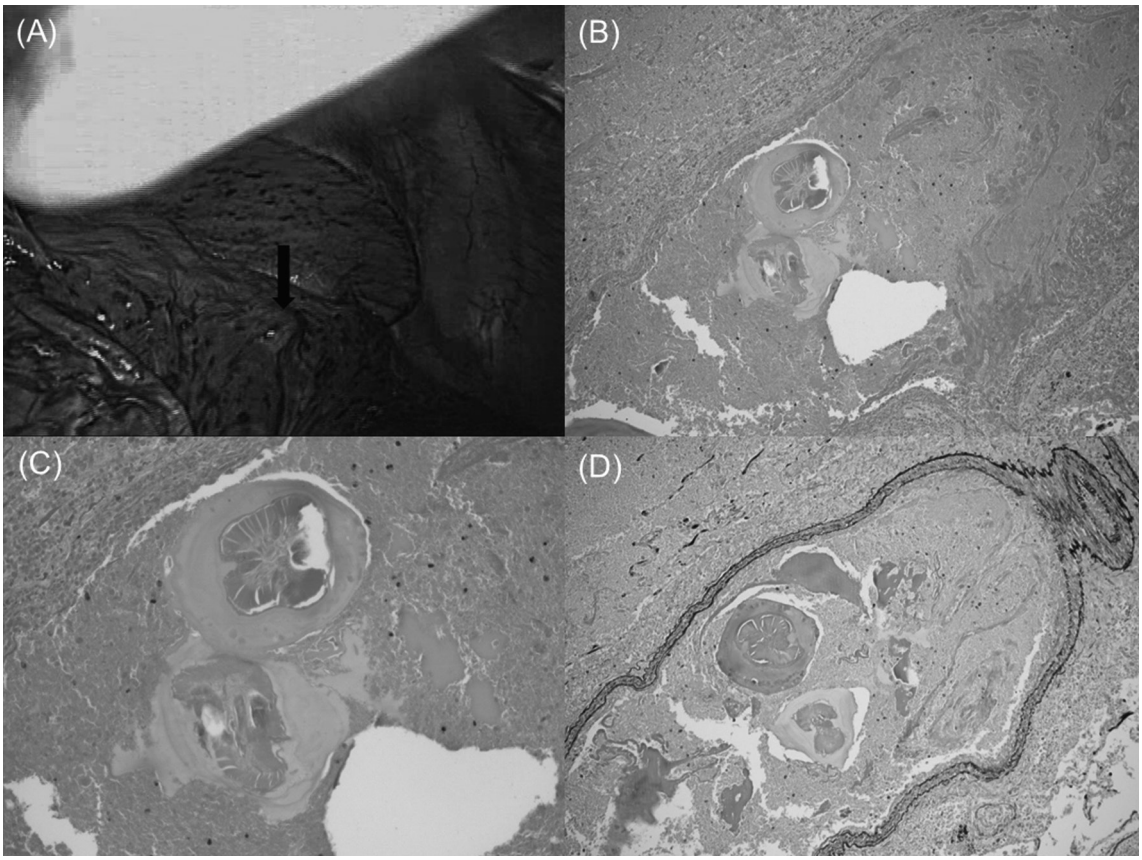

Fig. 2. (A) Operative finding of a tiny nodule (arrow) in the right middle lung. (B, C, D) Microscopic findings: Sections of the right middle lobe show a picture of infarction (B). Partial portions of larvae of nematode with a general body cavity, cuticle and subcuticle muscular layer (C) are noted in blood vessel lumen highlighted by elastic-Van Gieson stain (D). This was compatible with the diagnosis of pulmonary dirofilariasis based on the morphology.

bronchioloalveolar carcinomas and well-differentiated adenocarcinomas), small lesions, body weight, and uncontrolled hyperglycemia [8]. This explains why our patient, with a well-differentiated adenocarcinoma with a small size, had no obvious abnormal FDG uptake on PET/CT.

For a definitive diagnosis, surgical resection of pulmonary nodules remains the "gold standard". In operable patients with a single or small number of peripheral metastases, each of which is no greater than 3 cm in size, a wedge resection by VATS is the procedure of choice followed by a lobectomy [9]. In our case, the patient underwent wedge resection because of the poor pulmonary reserve, small size of the primary tumor, and possibly different etiology of the 2 nodules by image.

The life cycle of *Dirofilaria immitis* includes 5 larval stages, from the 1st-stage larvae (microfilariae), which are ingested by the mosquito, to the final 2 developmental stages, which are inoculated in the host, usually the dog's, subcutaneous tissue during the mosquito bite [10]. If the larvae migrate into the venous capillary channels, they are transmitted to the right ventricle and become adult worms, shedding microfilariae that can be detected in the periph-

eral blood smear of dogs. Humans are rarely infected by larvae-carrying mosquitoes during a blood meal, but when they are, the larvae never mature into fully gravid worms, so the human beings serve as dead-end reservoirs of the disease. The worms eventually die in the right ventricle, embolize into the pulmonary artery, and become organized into a necrotic and fibrotic nodule in the lung periphery, known as human pulmonary dirofilariasis [2,11].

The radiographic appearance of human pulmonary dirofilariasis is described typically as a solitary, well-circumscribed, non-calcified, subpleural "coin lesion" or nodule that is usually 1 to 3 cm in diameter and can be confused with a lung tumor. The spherical infarction caused by *Dirofilaria immitis* is reflected in the CT finding of central high attenuation and peripheral ground glass attenuation within the lesion [12]. Magnetic resonance imaging (MRI) revealed a low signal intensity of the nodule on both T1-weighted and T2-weighted imaging [13]. PET does not show the accumulation of FDG in the nodule [14]. Multiple nodules have also been reported in 10.2% of reviewed cases [4]. The differential diagnosis of these nodular lesions includes metastatic or benign tumors, caseous granulomatosis, histiocytosis, Wegener's granulomatosis, rheumatoid nodules and thromboembolism [2,15]. In a retrospective review of biopsied pulmonary lesions in 2908 cases, only 2 (0.06%) were caused by *Dirofilaria immitis* [16]. In our case, the small triangular opacity located peripherally reminded us of the possibility of pulmonary infarction.

The majority of patients are asymptomatic. In symptomatic cases, the most common symptom was cough (25%). Other symptoms, including fever, hemoptysis, and chest pain, were infrequent. A dog breeding history has been reported as having little relevance (only 25%) to infection [17].

Peripheral eosinophilia is commonly seen in many parasite infections. One study suggested an allergic inflammatory reaction, mediated by eosinophils and lymphocytes, was involved in the formation of the dirofilarial necrotizing granuloma, rather than infarction caused simply by embolism [18]. However, peripheral eosinophilia was noted in only 10% of patients with human pulmonary dirofilariasis [19]. Serological detection of human antibodies to dirofilariasis may be cross-reactive with other helminthes, and the value is also compromised by the length of time between the initial infection and the tests [17,20].

The definitive diagnosis requires histopathological examination. In the microscopic examination, the typical pulmonary nodule is well-circumscribed, grayish-yellow, and 1 to 3 cm in diameter. The larvae are usually found during cross-section of the nodules. Central necrosis surrounded by a granulomatous zone is found microscopically, and demarcated peripherally by fibrous tissue. The lung parenchyma contains scattered collections of lymphocytes, macrophages, and eosinophils. Pulmonary vessels reveal varying degrees of endarteritis [2,21].

The diagnostic method of choice is VATS because of its ability to identify the nodule reliably and with minimal invasiveness [17]. A thoracotomy with wedge resection is normally performed immediately after a solitary pulmonary nodule has been identified to rule out carcinoma. No treatment other than surgery is available for dirofilariasis, since it is not subject to microfilaraemia.

Conclusion

This is the first case report in Taiwan describing a rare instance of coexisting pulmonary dirofilariasis and lung cancer. Clinical suspicion of a mixed etiology should be maintained in a lung cancer patient with a separate lung nodule. An undetermined pulmonary nodule should not preclude the possibility of surgical intervention for lung cancer patients with resectable disease.

References

1. Wu CC, Fan PC. Prevalence of canine dirofilariasis in Taiwan. J Helminthol 2003; 77: 83-8.
2. Milanez de Campos JR, Barbas CS, Filomeno LT, *et al*. Human pulmonary dirofilariasis: analysis of 24 cases from Sao Paulo, Brazil. Chest 1997; 112: 729-33.
3. Theis JH. Public health aspects of dirofilariasis in the United States. Vet Parasitol 2005; 133: 157-80.
4. Ro JY, Tsakalakis PJ, White VA, *et al*. Pulmonary dirofilariasis: the great imitator of primary or metastatic lung tumor. A clinicopathologic analysis of seven cases and a review of the literature. Hum Pathol 1989; 20: 69-76.
5. Dashiell GF. A case of dirofilariasis involving the lung. Am J Trop Med Hyg 1961; 10: 37-8.
6. Yang SS WL, Fahn HJ. Solitary pulmonary nodule caused by dirofilariasis immitis. A case report and literature review. Surg Assoc Roc 1993; 26: 1713-8.
7. Ginsberg MS GS, Go BD, Yoo HH, *et al*. Pulmonary nodules resected at video-assisted thoracoscopic surgery: etiology in 426 patients. Radiology. 1999 213(1): 277-82.
8. Iwano S, Ito S, Tsuchiya K, *et al*. What causes false-negative PET findings for solid-type lung cancer? Lung Cancer 2013; 79: 132-6.
9. Tan BB, Flaherty KR, Kazerooni EA, *et al*. The solitary pulmonary nodule. Chest 2003; 123: 89S-96S.
10. Orihel TC. Morphology of the larval stages of *Dirofilaria immitis* in the dog. J Parasitol 1961; 47: 251-62.
11. HG. S. Migrating worms. In: Stephen HG, Richard DP (eds). Principle and Practice of Clinical Parasitology. John Wiley and Sons, Chichester, 2001: 535-51.
12. Wand A, Kasirajan LP, Sridhar S, *et al*. Solitary pulmonary nodule due to dirofilariasis. J Thorac Imaging 2000; 15: 198-200.
13. Oshiro Y, Murayama S, Sunagawa U, *et al*. Pulmonary dirofilariasis: computed tomography findings and correlation with pathologic features. J Comput Assist Tomogr 2004; 28: 796-800.
14. Terasaka Y, Inaba H, Furuta S, *et al*. Human pulmonary dirofilariasis. Kyobu Geka 2011; 64: 1096-9.
15. Patel D, Doi K. Images in medicine. Human pulmonary dirofilariasis. Med Health R I 2003; 86: 80.
16. Rolston KV, Rodriguez S, Dholakia N, *et al*. Pulmonary infections mimicking cancer: a retrospective, three-year review. Support Care Cancer 1997; 5: 90-3.
17. Miyoshi T, Tsubouchi H, Iwasaki A, *et al*. Human pulmonary dirofilariasis: a case report and review of the recent Japanese literature. Respirology 2006; 11: 343-7.
18. Araya J, Kawabata Y, Tomichi N, *et al*. Allergic inflammatory reaction is involved in necrosis of human pulmonary dirofilariasis. Histopathology 2007; 51: 484-90.
19. Flieder DB, Moran CA. Pulmonary dirofilariasis: a clinicopathologic study of 41 lesions in 39 patients. Hum Pathol 1999; 30: 251-6.
20. Sun S, Sugane K. Immunodiagnosis of human dirofilariasis by enzyme-linked immunosorbent assay using recombinant DNA-derived fusion protein. J Helminthol 1992; 66: 220-6.
21. Asimacopoulos PJ, Katras A, Christie B. Pulmonary dirofilariasis. The largest single-hospital experience. Chest 1992; 102: 851-5.

肺癌病患合併人體肺部犬心絲蟲症－病例報告

蕭逸函　馮嘉毅　吳玉琮 *　葉奕成 **　李毓芹　邱昭華

犬心絲蟲症乃流浪狗之中常見之寄生蟲感染。在極罕見之情況下，蟲體可藉由中間宿主－蚊子，在人體肺部形成病灶。影像學上，典型的病灶為邊緣完整，位於周邊之孤立性結節，常與肺部癌症造成混淆。必須依賴手術切除後，顯微鏡下看見部分蟲體的病理發現才能診斷。在本文中，我們報告一位 48 歲女性在診斷肺癌的同時，意外發現肺部犬心絲蟲病灶。臨床上若在肺癌病患見到腫瘤以外之肺部結節，應考慮腫瘤肺部轉移以外之診斷。若病患可接受手術切除，術前無法診斷之肺部結節應考慮切除以達成適當之診斷。*(胸腔醫學 2014; 29: 85-91)*

關鍵詞：肺部犬心絲蟲症，肺癌，孤立性肺結節

台北榮民總醫院　胸腔部，台北榮民總醫院　外科部　胸腔外科 *，台北榮民總醫院　病理檢驗部 **
索取抽印本請聯絡：邱昭華醫師，台北榮民總醫院　胸腔部，台北市北投區石牌路二段 201 號

Interstitial Pneumonitis Suspected as a Consequence of Interferon Therapy for Hepatitis C: Case Report

Ching-Shan Luo, Guang-Ming Shiao

Since the year 2004, the combination of pegylated interferon (IFN) with ribavirin has been the treatment of choice for chronic hepatitis C virus (HCV) infection. Though potentially effective, pegylated IFN and ribavirin are known to have various side effects in HCV patients. Interstitial pneumonitis (IP) occurs only rarely as a side effect of this kind of therapy. However, with the increasing use of the therapy, more and more IP cases will present in the future. We report a 71-year-old man who developed IP during IFN alfa treatment. Fever and chills were noted beginning in the last month (the 11th month) of IFN treatment. Productive cough with whitish sputum, dyspnea on exertion and poor appetite were also noted. A diagnosis of suspected IFN-induced IP was made based on the negative results of the pathogen survey, chest radiography, high resolution computed tomography and bronchoalveolar lavage fluid analysis. He was treated with oral prednisolone and the clinical symptoms and pulmonary infiltrates resolved markedly. Physicians should be aware of this rare but possibly severe pulmonary complication of IFN treatment in order to prevent further pulmonary damage and mortality. HCV infection follow-up is also needed in cases of HCV infection reactivation or progression if immunosuppressive agents are used for IP treatment. ***(Thorac Med 2014; 29: 92-99)***

Key words: hepatitis C virus, interferon, ribavirin, interstitial pneumonitis

Introduction

Since the year 2004, the combination of pegylated interferon (IFN) with ribavirin has been the treatment of choice for chronic hepatitis C virus (HCV) infection because of its recommendation by the American Association for the Study of Liver Disease [1]. Attaching polyethylene glycol to a protein (pegylation) reduces its rate of absorption after subcutaneous injection, reduces renal clearance, and decreases the immunogenicity of the protein. All of these effects can prolong the half-life of pegylated IFN and provide a more sustained anti-virus effect than conventional IFN [2]. Though potentially effective, pegylated IFN and ribavirin are known to have various side effects in HCV patients; of these, interstitial pneumonitis (IP) occurs only rarely [3-8]. However, as the use of the therapy increases, more and more IP cases will present in the future. We report a 71-year-old man who developed IP during IFN alfa treatment. The

Department of Chest Medicine, Taipei Veterans General Hospital, Taipei, Taiwan
Address reprint requests to: Dr. Guang-Ming Shiao, Department of Chest Medicine, Taipei Veterans General Hospital, #201, Section 2, Shih-Pai Road, Taipei 11217, Taiwan

disease was treated successfully with oral prednisolone.

Case Report

A 71-year-old man received pegylated interferon alfa-2a 180 mg subcutaneous injection once weekly plus ribavirin 600 mg orally twice daily for treatment of hepatitis C virus infection for 1 year. Fever up to 38 degrees Celsius and chills accompanied with shortness of breath were noted beginning in the last month of treatment. Productive cough with whitish sputum, dyspnea on exertion and poor appetite were also noted. He denied having cold sweating, orthopnea, abdominal discomfort or rash. He was a never-smoker, and there was no occupational exposure (he was a retired pediatrist), no recent travel history and no special animal contact in the last 6 months. He also denied having autoimmune disease and a specific drug history. Because of the symptoms and signs described above, he was admitted to another hospital about 1 month prior to coming to our institution under the impression of atypical pneumonia. He received empirical parenteral antibiotics such as amoxicillin/clavulanic acid, levofloxacin and piparacillin, but his symptoms persisted. He was then transferred to our hospital (about 1 month after the completion of INF therapy) for further evaluation.

Upon arrival, his vital signs were as follows: heart rate 96/min, respiratory rate 20/min, blood pressure 122/72 mmHg, and body temperature 37 degrees Celsius. Physical examination showed bilateral mild inspiration crackles without wheezing. The HCV viral load was undetectable, and his serum aspartate transaminase (AST) and alanine transaminase (ALT) were within normal limits. Other laboratory data showed: white blood cells (WBC) 3700/μl, hemoglobin (Hb) 8.3 g/dl, platelets 167000/μl, segments 73.7%, lymphocytes 13.2%, monocytes 9.2%, eosinophils 3.6%, basophils 0.3% and C-reactive protein 9.76 mg/dl. Chest radiography revealed increased interstitial opacities in bilateral lung fields (Figure 1). High resolution computed tomography (HRCT) revealed consolidation and a ground glass appearance at the bilateral lower lungs and right middle lung (Figure 2). The patient received cefepime and teicoplanin initially as empirical treatment, but the symptoms of intermittent low-grade fever persisted. Serology tests for atypical and fungal pathogens, including *Mycoplasma pneumoniae*, *Legionella pneumophila*, *Chlamydophylla pneumoniae*, Cryptococcus and Aspergillus, were all negative. Acid-fast bacilli were not found in the sputum and sputum culture showed no growth of bacteria. Cytomegalovirus (CMV) RNA was undetectable by polymerase chain reaction (PCR) assay, and the (enzyme-linked immunosorbent assay) ELISA screen test for

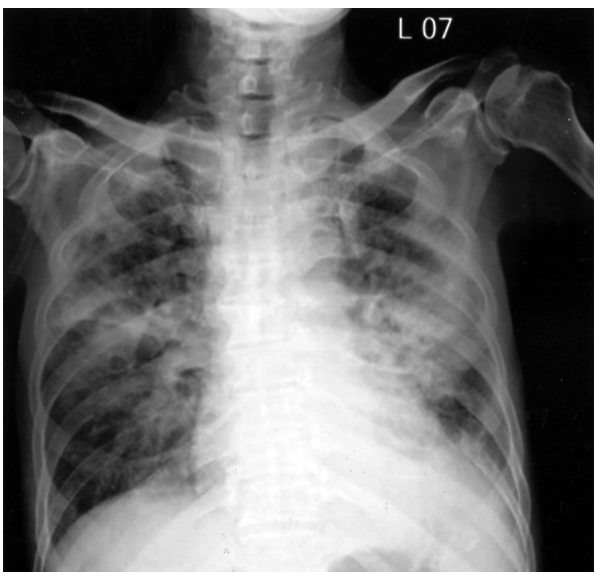

Fig. 1. Chest radiography on the day of admission showed increased interstitial opacities in bilateral lung fields.

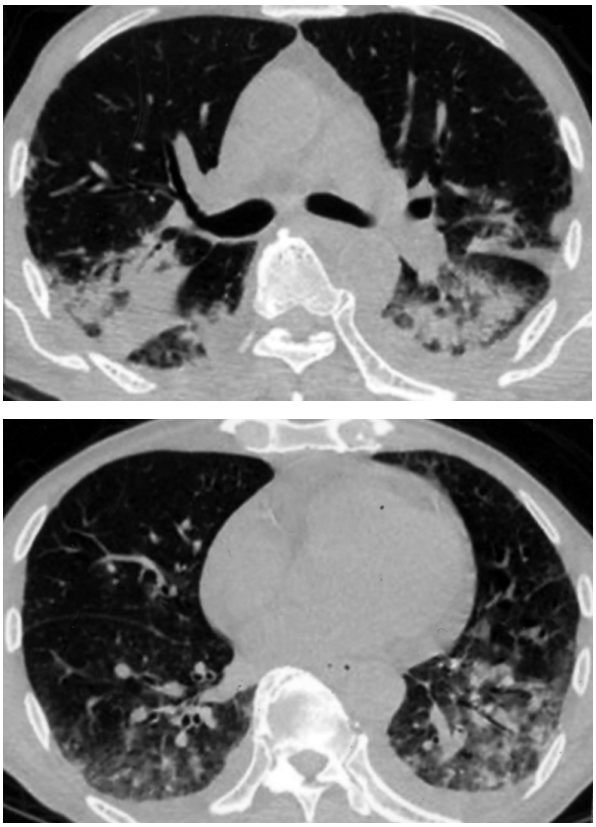

Fig. 2. High resolution computed tomography (HRCT) revealed consolidation and a ground glass appearance at the bilateral lower lungs and right middle lung.

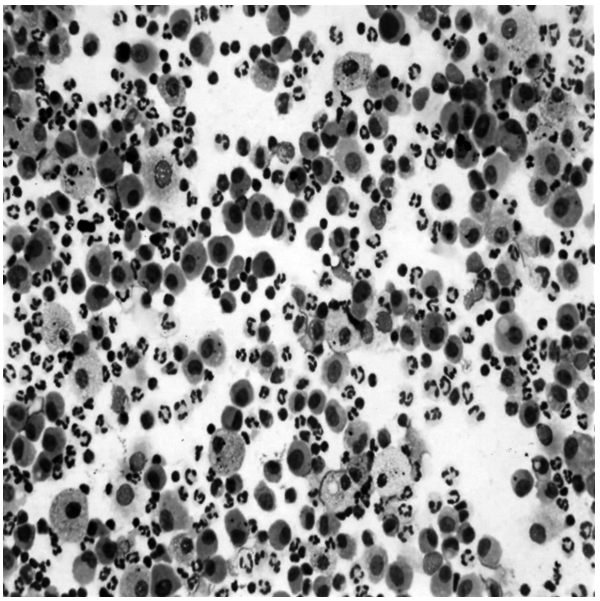

Fig. 3. Liu satin of bronchoalveolar lavage fluid showed increased neutrophil and lymphocyte counts. (x400)

human immunodeficiency virus (HIV) also revealed a negative result. Immunological examinations revealed negative anti-nuclear antibody, positive anti-SSA antibody, positive Schirmer test and advanced xerostomia by sialoscintigraphy. However, there was no symptom of dry eyes or dry mouth. The diagnosis of primary Sjögren's syndrome was not made based on the available data [10]. Bronchoalveolar lavage (BAL) was performed, and BAL fluid analysis demonstrated that the number of lymphocytes and neutrophils was increased (Figure 3). Culture and staining of BAL fluid were negative for bacteria, fungi, acid-fast bacilli and viruses. The complaints of low-grade fever and shortness of breath persisted and follow-up chest radiography showed disease progression after 12 days of empirical antibiotics (Figure 4). Under the impression of suspected INF treatment-related IP, prednisolone 20 mg orally once daily was started. His fever subsided and shortness of breath also gradually subsided. The pulmonary infiltrates on chest radiography showed regressive change 5 days after the steroid treatment (Figure 5). The patient was discharged after 20 days of steroid treatment in a stable condition. The steroid was tapered out gradually 2 months after discharge, and follow-up chest radiography showed marked improvement (Figure 6).

Discussion

The effects of IFN alfa include antiviral activity, growth regulation, inhibition of angiogenesis, regulation of cell differentiation, enhancement of the expression of major histocompatibility complex antigens, enhancement of the activity of natural killer cells and cyto-

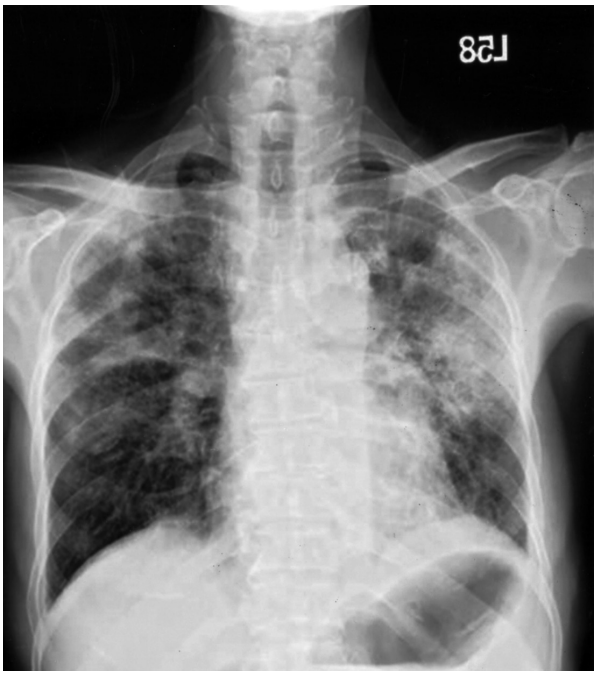

Fig. 4. Chest radiography showed disease progression after 12 days of empirical antibiotics treatment.

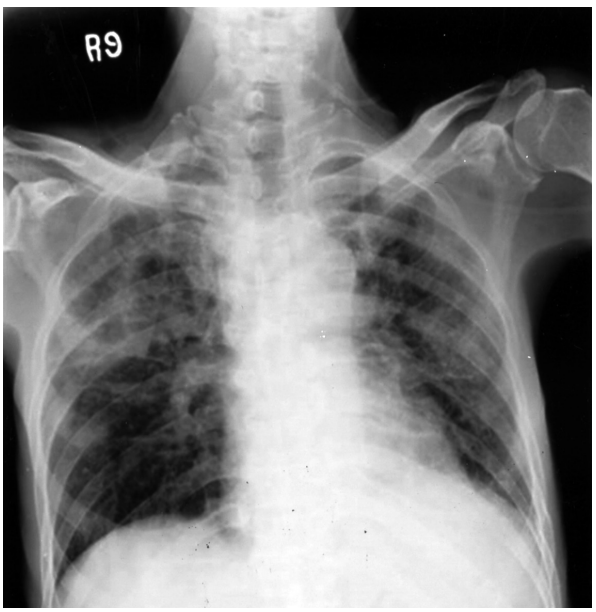

Fig. 5. Chest radiography also showed regressive change 5 days after the steroid treatment.

toxic T lymphocytes, and increased expression of class I and II human leukocyte antigens [11]. Despite its great anti-HCV activity, IFN alfa

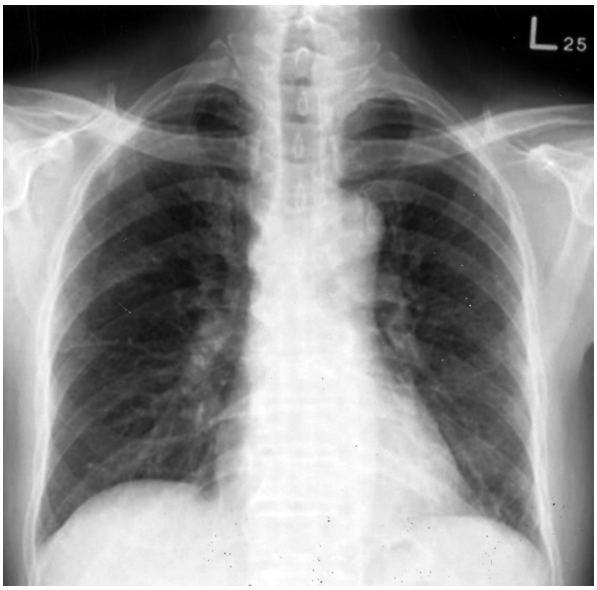

Fig. 6. Chest radiography showed marked improvement when steroid was tapered out after 3 months' treatment.

has some well-known side effects, such as a flu-like syndrome (fever, chills, tachycardia, malaise, myalgia, and headache), leukopenia, thrombocytopenia, depression, seizures, thyroid dysfunction, alopecia and activation of buccal lichen planus [12]. Pulmonary toxicities, including sarcoidosis, bronchiolitis obliterans organizing pneumonia, pleural effusion, IP and exacerbation of bronchial asthma, are rare, but may occur after long-term usage [6,13-14]. The possible mechanisms for IFN pulmonary toxicity include inhibition of suppressor T cells, enhancement of cytotoxic T cells, induction of proinflammatory cytokines, and exaggerated release of fibrinogenic cytokines [6]. It is thought that IFN induces a lung-specific immune-mediated response resulting in IP, similar to other autoimmune diseases [7]. IFN toxicity is generally dose- and duration-dependent [14]. Therefore, pulmonary toxicity may occur more frequently with longer-acting and higher blood levels of pegylated IFN alfa therapy compared with conventional IFN therapy. In addition,

HCV itself may play a cooperative role in the pathogenesis of IP [15]. Although side effects of ribavirin such as dose-dependent hemolytic anemia, rash, depression, cough and dyspnea may develop, until now there has been no case report of IP with ribavirin use alone [5,7].

The overall incidence of pulmonary toxicities is < 1% [6], and the incidence rate of IP is estimated to be 0.01-0.3% [5]. However, with the increasing use of IFN, more and more IP cases will present. Ji *et al*. reported that the mean IFN treatment time before the diagnosis of IP was 11.8 weeks (range 2-48 weeks) [5]. Onset of IP at any stage of HCV treatment implies the idiosyncratic nature of this side effect [7]. The clinical presentation of IP is usually insidious in onset. Differential diagnoses include a transient viral respiratory disease, atypical pneumonia, congestive heart failure and ribavirin-induced cough and dyspnea. Symptoms of dyspnea, dry cough, fever, fatigue, arthralgia or myalgia, and anorexia may develop. Hemoptysis, wheezing and signs of consolidation are rare. Physical examination mostly reveals unilateral or bilateral lung field fine crackles. Pulmonary function test may show a restrictive pulmonary function impairment pattern. Chest radiographs usually show bilateral patchy infiltration or opacities, and HRCT may show bilateral patchy consolidation as well as ground-glass attenuation [5-7]. BAL fluid analysis with a pattern of lymphocytes, neutrophils, and eosinophils, or a mixed cellular pattern can be used as an adjunct to diagnosis [5]. A biopsy was considered positive for IP when histology demonstrated principally lymphocyte and macrophage interstitial infiltration, and interstitial fibrosis with thickening of alveolar walls and without evidence of granulomatous lesions in the parenchyma [5]. In our case, the symptoms and signs of dyspnea and fever were noted beginning about 44 weeks after INF treatment. Infectious disease of the lung was excluded by sputum and BAL fluid cultures. The image studies and BAL fluid cell analysis supported the diagnosis of IP induced by IFN.

The key points in the management of IP associated with IFN therapy are to recognize the disease, stop usage of the offending agent immediately, and provide the best supportive care [3,5-7]. In some patients, IP resolved without treatment, while others required treatment with steroids or other agents. The dosage and length of steroid use are highly variable; it is usually started at a relatively high dosage and gradually tapered for weeks. A 39-year-old female IP patient was treated with methylprednisolone 160 mg/day for 3 days and 80 mg/day for 4 days, followed by prednisolone 30 mg daily, with the dosage gradually tapered over the next 12 weeks [16]. Another 56-year-old male patient was treated with methylprednisolone 2 g/day for 3 days and prednisolone 40 mg/day for 2 days [17]. Prednisolone 60 mg daily and azathioprine 100 mg daily were given after a relapse of IP that was initially treated with prednisolone 30 mg daily [18]. Plasmapheresis therapy may be the 3rd-line alternative choice to remove humoral factors and proinflammatory and fibrinogenic cytokines from the circulation, which may decrease host IFN response-associated pulmonary activity and toxicity [3]. In our case, prednisolone 20 mg daily was given immediately after IP was diagnosed by the negative pathogen culture result, failure of the empirical antibiotics trial, and adjunct BAL fluid cell analysis. The patient recovered as a result of the therapy.

Slavenburg *et al*. reported a mortality rate of 7% (4 of 58 patients) in IFN-induced IP [7].

All patients had been treated with pegylated IFN alfa-2b. Causes of death included multiple organ failure, cerebral edema and acute cholestatic hepatitis. No deaths were due to purely respiratory failure.

Immunological examination results in our case fulfilled 3 of the objective Sjögren's syndrome classification criteria (positive anti-SSA antibody, positive Schirmer test and advanced xerostomia by sialoscintigraphy). Diagnosis of the disease is normally made once another histopathological criterion is confirmed [10]; however, our patient did not receive a minor salivary gland biopsy, so there is the possibility that the patient had Sjögren's syndrome. It is well known that IP is a respiratory complication of Sjögren's syndrome, with an estimated incidence rate of 25% [19-20]. However, since these symptoms and signs of Sjögren's syndrome in patients with HCV infection might just be considered as extrahepatic manifestations of the HCV infection, the diagnosis of primary Sjögren's syndrome (PSS) would require more laboratory data and follow-up observations [9-10]. There was no IP relapse in the outpatient department follow-up of our patient after the steroid was tapered out. This may be indirect evidence that the IP was caused by IFN instead of PSS, which would less likely be cured by low-dose steroid. On the other hand, HCV itself may also cause IP [15] (another extrahepatic manifestation), but this was less likely in our case since the HCV viral load was undetectable when IP was diagnosed.

HCV infection reactivation (viral load 22,000,000 IU/mL by RT-PCR) was noted after 2 months of oral prednisolone treatment in our patient, despite improvement in pulmonary symptoms and signs. Therefore, HCV infection follow-up is also needed in case of HCV infection reactivation or progression if an immunosuppressive agent was used for IP treatment.

Conclusion

IP is a rare pulmonary complication associated with IFN therapy for HCV infection. However, since the optimal treatment for chronic HCV infection at the present time is a combination of pegylated IFN alfa with ribavirin, HCV may occur more frequently in the future. Physicians should be aware of this rare but possibly severe complication in order to prevent further pulmonary damage and mortality. HCV infection follow-up is also needed in case of reactivation or progression when an immunosuppressive agent is used for IP treatment.

References

1. Strader DB, Wright T, Thomas DL, *et al*. Diagnosis, management, and treatment of hepatitis C. Hepatology 2004; 39: 1147-71.
2. Shiffman ML. Pegylated interferons: what role will they play in the treatment of chronic hepatitis C? Curr Gastroenterol Rep 2001; 3: 30-7.
3. Carrillo-Esper R, Gonzalez-Avila D, Uribe-Rios M, *et al*. Interstitial pneumonitis associated with pegylated interferon alpha-2b therapy for chronic hepatitis C: case report. Ann Hepatol 2008; 7: 87-90.
4. Chen YC, Lu SN, Lin MC. Interstitial pneumonitis after combination therapy with pegylated interferon alpha-2b and ribavirin for chronic hepatitis C. Chang Gung Med J 2007; 30: 92-7.
5. Ji FP, Li ZX, Deng H, *et al*. Diagnosis and management of interstitial pneumonitis associated with interferon therapy for chronic hepatitis C. World J Gastroenterol 2010; 16: 4394-9.
6. Midturi J, Sierra-Hoffman M, Hurley D, *et al*. Spectrum of pulmonary toxicity associated with the use of interferon therapy for hepatitis C: case report and review of the literature. Clin Infect Dis 2004; 39: 1724-9.

7. Slavenburg S, Heijdra YF, Drenth JP. Pneumonitis as a consequence of (peg)interferon-ribavirin combination therapy for hepatitis C: a review of the literature. Dig Dis Sci 2010; 55: 579-85.
8. Vartany E, Caldwell CA, Trow TK. Adult respiratory distress syndrome after treatment with pegylated interferon alpha-2a and ribavirin. Heart Lung 2008; 37: 153-6.
9. Ramos-Casals M, Munoz S, Zeron PB. Hepatitis C virus and Sjogren's syndrome: trigger or mimic? Rheum Dis Clin North Am 2008; 34: 869-84.
10. Vitali C, Bombardieri S, Jonsson R, *et al*. Classification criteria for Sjogren's syndrome: a revised version of the European criteria proposed by the American-European Consensus Group. Ann Rheum Dis 2002; 61: 554-8.
11. Wang YS, Youngster S, Grace M, *et al*. Structural and biological characterization of pegylated recombinant interferon alpha-2b and its therapeutic implications. Adv Drug Deliv Rev 2002; 54: 547-70.
12. Fontaine H, Pol S. Side effects of interferon-alpha in treating hepatitis C virus infection. Transplant Proc 2001; 33: 2327-9.
13. Kumar KS, Russo MW, Borczuk AC, *et al*. Significant pulmonary toxicity associated with interferon and ribavirin therapy for hepatitis C. Am J Gastroenterol 2002; 97: 2432-40.
14. Tahan V, Ozseker F, Guneylioglu D, *et al*. Sarcoidosis after use of interferon for chronic hepatitis C: report of a case and review of the literature. Dig Dis Sci 2003; 48: 169-73.
15. Aliannejad R, Ghanei M. Hepatitis C and pulmonary fibrosis: Hepatitis C and pulmonary fibrosis. Hepat Mon 2011; 11: 71-3.
16. Ji FP, Li ZX, Deng H, *et al*. Clinical features of interstitial pneumonitis due to interferon alpha therapy for chronic hepatitis C. Nan Fang Yi Ke Da Xue Xue Bao 2009; 29: 667-70.
17. Chin K, Tabata C, Sataka N, *et al*. Pneumonitis associated with natural and recombinant interferon alfa therapy for chronic hepatitis C. Chest 1994; 105: 939-41.
18. Hizawa N, Kojima J, Kojima T, *et al*. A patient with chronic hepatitis C who simultaneously developed interstitial pneumonia, hemolytic anemia and cholestatic liver dysfunction after alpha-interferon administration. Intern Med 1994; 33: 337-41.
19. Constantopoulos SH, Papadimitriou CS, Moutsopoulos HM. Respiratory manifestations in primary Sjogren's syndrome. A clinical, functional, and histologic study. Chest 1985; 88: 226-9.
20. Segal I, Fink G, Machtey I, *et al*. Pulmonary function abnormalities in Sjogren's syndrome and the sicca complex. Thorax 1981; 36: 286-9.

疑似以干擾素治療 C 型肝炎後造成的間質性肺炎：病例報告

羅青山　蕭光明

自 2004 年左右，長效型干擾素合併 ribavirin 已經成為治療慢性 C 型肝炎的最佳選擇藥物。雖然成效不錯，但是干擾素及 ribavirin 都各自有不同已知的副作用。間質性肺炎是此合併治療一種罕見的副作用。但是隨著此種治療方法的普遍採用，在未來將會有越來越多的間質性肺炎案例發生。我們提出一個 71 歲男性接受長效型干擾素合併 ribavirin 治療後發現間質性肺炎的案例。病人在治療的最後一個月（第 11 個月）開始產生發燒及發冷的症狀，伴隨症狀有白色有痰性咳嗽、活動性呼吸困難及食慾減弱。根據陰性病原菌檢查結果、胸部 X 光、胸部高解析電腦斷層及支氣管肺泡灌洗液分析結果，病人被診斷為疑似干擾素引發之間質性肺炎。經給予口服類固醇治療後，臨床症狀及影像上肺部浸潤皆有顯著改善。臨床醫師必須對干擾素治療後此種罕見但嚴重的肺部副作用有所警覺，以期及早介入並避免進一步的肺損傷和致死性。若使用免疫抑制劑治療此種間質性肺炎，必須定期追蹤 C 型肝炎病毒量以早期發現 C 型肝炎復發或惡化。*(胸腔醫學 **2014; 29: 92-99**)*

關鍵詞：C 型肝炎，干擾素，ribavirin，間質性肺炎

台北榮民總醫院　胸腔部
索取抽印本請聯絡：蕭光明醫師，台北榮民總醫院　胸腔部，11217 台北市北投區石牌路二段 201 號

Missed Tumor with Chest Pain: Subtle Pleural Metastasis in Primary Adenocarcinoma of the Lung

Chia-Hsin Liu, Chih-Feng Chian, Wann-Cherng Perng, Chen-Liang Tsai

Subtle pleural metastasis without pleural effusion in patients with primary lung cancer may be misdiagnosed as operable, resulting in an inaccurate clinical staging. We report a case of a 48-year-old woman presenting with a 1-month history of right lower chest pain with an initial negative chest radiography finding. Chest CT showed a 2.2-cm nodule in the medial right lower lobe adherent to the adjacent pleura, with slight pleural thickness and irregularity but without pleural effusion. Transthoracic needle biopsy showed moderately differentiated primary pulmonary adenocarcinoma. Nevertheless, video-assisted thoracic surgery showed multiple nodules in the ipsilateral, parietal, and visceral pleura. Histopathology revealed the nodules were metastatic, poorly differentiated adenocarcinomas from the lung. ***(Thorac Med 2014; 29: 100-104)***

Key words: missed cancer, chest pain, pleural metastasis, adenocarcinoma

Introduction

Chest pain is the leading symptom of patients visiting pulmonology clinics. Chest radiography (CXR) is the imaging modality used in the detection of lung cancer at both early and late stages. However, a previous study has highlighted the problem of "missed" lung cancers on CXR [1]. Potentially resectable non-small cell lung cancer (NSCLC) lesions that were missed on CXR had been overlooked on the film. Many of the overlooked cancers were very difficult to see, even in retrospect [2]. Pleural metastases are considered indicators of a poor prognosis, rendering the tumor inoperable. Patients with pleural metastases present with a variety of clinical signs and symptoms. Subtle pleural metastasis without pleural effusion may be misdiagnosed as operable, resulting in unnecessary thoracotomy. Herein, we report the case of a patient with NSCLC presenting with chest pain and a lesion missed on the initial CXR. The subtle pleural metastasis was diagnosed finally by video-assisted thoracic surgery (VATS).

Division of Pulmonary and Critical Care Medicine, Department of Internal Medicine, Tri-Service General Hospital, National Defense Medical Center, Taipei, Taiwan
Address reprint requests to: Dr. Chen-Liang Tsai, Division of Pulmonary and Critical Care Medicine, Department of Internal Medicine, Tri-Service General Hospital, National Defense Medical Center, 325, Section 2, Cheng-Gung Road, Nei-Hu Dist. 114, Taipei, Taiwan, Republic of China

Case Report

A 48-year-old woman presented with a 1-month history of right lower chest pain. The pain was localized primarily at the posterolateral aspect of the right seventh inter-costal space and worsened with coughing and sneezing. Initial CXR showed no significant abnormal finding, so a non-steroidal anti-inflammatory drug was prescribed for 1 week for symptom control (Figure 1). However, the chest pain persisted and the patient was only partially relieved. Chest computed tomography (CT) was ordered and revealed a 2.2-cm nodule in the paravertebral region of the right lower lobe adhering to the adjacent pleura. Following CT-guided fine needle tumor biopsy, a moderately differentiated adenocarcinoma was confirmed (Figure 2A). The staging exams, such as brain MRI, whole body bone and whole abdominal sonography, found no occult metastatic lesions. PET/CT showed a solitary FDG-avid lesion with early and delayed SUVmax of 10.4 and 15, respectively, at the corresponding site observed on CT, but no other evidence of abnormal uptake. The tumor was initially staged as stage cT1bN0M0, stage IA. However, considering the patient's chest pain, we reviewed the chest CT, and the subtle pleural lesions aroused our suspicion (Figure 2B). VATS was indicated for further confirmation of metastasis. The operation findings revealed a tumor in the superior segment of the right lower lobe, involving the posterior segment of the right upper lobe, with numerous seed-like small tumors implanted in the adjacent parietal and visceral pleura (Figure 2C, D). Resection of the parietal pleura with pleurodesis was performed by VATS. Histology revealed that these lesions were compatible with metastatic adenocarcinoma from the lung, with subsequent pathologic staging ultimately revealing pT2N0M1a, stage IV cancer.

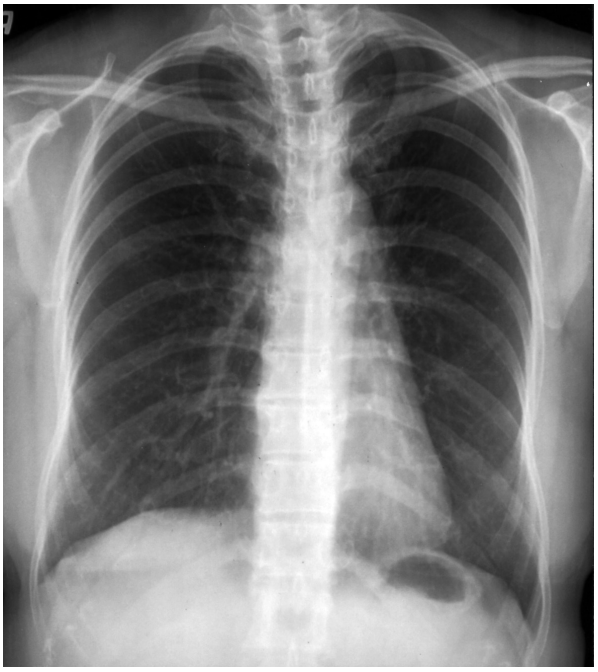

Fig. 1. CXR revealed no significant abnormal finding.

Discussion

It has been reported that in general radiologic practice, bronchogenic carcinomas are missed on CXR in 19% of cases [1-2]. The miss rate was particularly high in CXR lung cancer screening programs, a particular setting involving the opportunity to undertake meticulous review of recent films. Potentially resectable NSCLC lesions missed on CXR were characterized by predominantly peripheral (85%) and upper lobe (72%) locations and by apical and posterior segmental/sub-segmental locations in the upper lobe (60%) [2].

Adenocarcinoma is the most common histologic type of lung cancer causing pleural metastasis [3], with most patients usually presenting with dyspnea and cough due to pleural effusion.

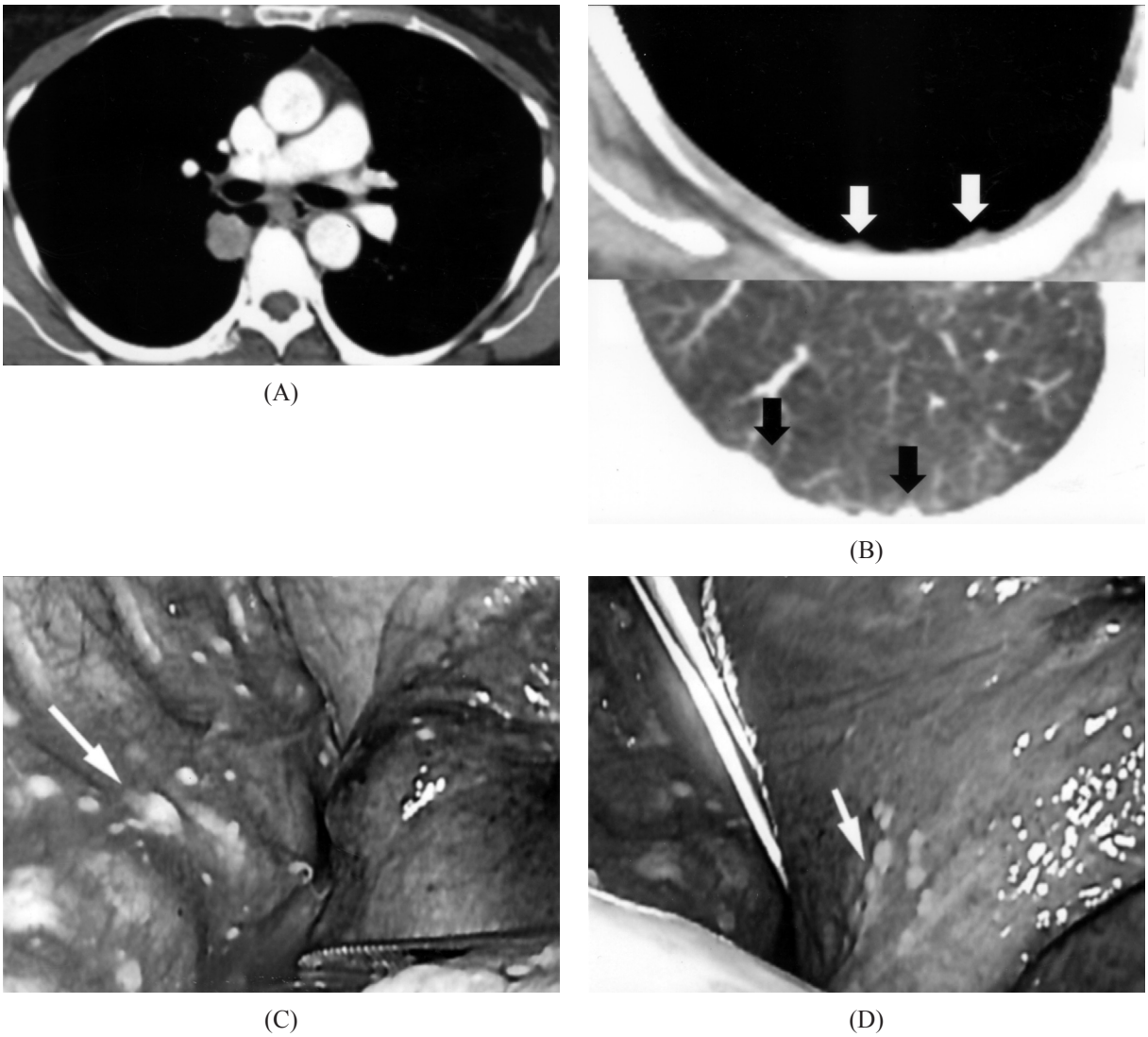

Fig. 2. A, Chest CT scan shows a 2.2-cm nodule in the paravertebral region of the right lower lobe adhering to the adjacent pleura. B, Review of chest CT scan showing slight pleural thickening and irregularity (arrows) without pleural effusion. C, D, VATS findings of tumor seeding along the adjacent parietal (long arrow) and visceral (short arrow) pleura.

Although only one-fourth of patients with pleural metastasis experience chest pain, severe, persistent, and localized pain usually indicates parietal pleural involvement and may be an early manifestation of subtle pleural metastasis [4]. Pleural metastasis may present on chest CT as slight ipsilateral pleural thickening or nodularity adjacent to the primary tumor [4]. Retrospective review of preoperative chest CT scans has shown that subtle pleural metastases may be caused by the primary tumor abutting an adjacent interlobar fissure, or a mediastinal or costal pleural surface [5]. Subtle pleural metastasis without pleural effusion may be due to exfoliation from tumors abutting the pleural surface or tumor invasion of subpleural lymphatics. In this case, the primary tumor was located in the right lower lobe abutting the medial costal pleural

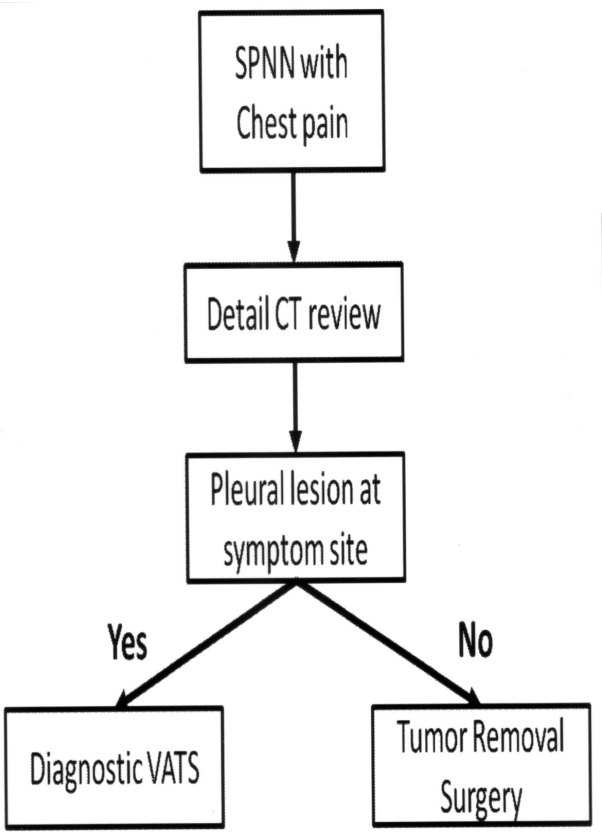

Fig. 3. Suggested diagnostic algorithm for patients with a solitary pulmonary neoplastic nodule (SPNN) and chest pain.

surface, possibly contributing to subtle pleural metastasis. If pleural abnormalities are unclear, pathologic confirmation is required for a final diagnosis.

Herein, we reported a case of lung adenocarcinoma presenting with chest pain and an initial negative CXR. The subtle pleural change, which was difficult to discern on the initial chest CT, turned out to be pleural metastasis. We have proposed a diagnostic flow chart to improve the clinical lung cancer staging process in patients with a solitary pulmonary neoplastic nodule (SPNN) and chest pain (Figure 3). If patients with SPNN have chest pain, a thorough chest CT assessment should be carried out to detect vague parietal pleural lesions. If no pleural lesions are identified, tumor removal surgery is suggested. If pleural lesions at a symptomatic site are identified, VATS may be helpful for diagnostic confirmation.

In conclusion, in cases of idiopathic chest pain and initial non-diagnostic CXR, chest CT is indicated to detect possible hidden lesions, such as missed cancer. In possibly resectable NSCLC patients presenting with unexplained chest pain, a detailed CT parietal pleura review is essential for clinicians to avoid missing subtle pleural metastasis, and VATS may be useful for diagnostic proof.

Acknowledgements

We would like to thank Miss Jennifer for providing image typesetting assistance.

References

1. Austin JH, Romney BM, Goldsmith LS. Missed bronchogenic carcinoma: radiographic findings in 27 patients with a potentially resectable lesion evident in retrospect. Radiology 1992; 182(1): 115-22.
2. Shah PK, Austin JH, White CS, *et al*. Missed non-small cell lung cancer: radiographic findings of potentially resectable lesions evident only in retrospect. Radiology 2003; 226(1): 235-41.
3. Chernow B, Sahn SA. Carcinomatous involvement of the pleura: an analysis of 96 patients. Am J Med 1977; 63(5): 695-702.
4. Hwang JH, Song KS, Park SI, *et al*. Subtle pleural metastasis without large effusion in lung cancer patients: preoperative detection on CT. Korean J Radiol 2005; 6(2): 94-101.
5. Kjellberg SI, Dresler CM, Goldberg M. Pleural cytologies in lung cancer without pleural effusions. Ann Thorac Surg 1997; 64(4): 941-4.

胸部 X 光遺漏的病灶合併胸痛：原發性肺腺癌合併細微肋膜轉移

劉佳鑫　簡志峯　彭萬誠　蔡鎮良

原發性肺癌患者合併難以辨識肋膜轉移而無肋膜積液，可能會造成不準確的臨床分期，而進行傳統開胸手術。我們的案例報告是一個 48 歲的女性右下胸痛持續約 1 個月，而且一開始的胸部 X 光檢查是正常的。胸部電腦斷層顯示右下肺葉內側一個約 2.2 厘米鄰近肋膜肺結節，腫瘤穿刺結果為原發性肺腺癌。於患側合併有非典型細微肋膜增厚及不規則，且無肋膜積液。胸腔內視鏡輔助手術（VATS）顯示右側壁層及臟層肋膜呈現多發性結節，組織病理學檢查結果為低度分化的轉移性肺腺癌。*(胸腔醫學* ***2014; 29: 100-104)***

關鍵詞：遺漏肺癌，胸痛，肋膜轉移，肺腺癌

三軍總醫院　內科部　胸腔內科
索取抽印本請聯絡：蔡鎮良醫師，三軍總醫院　胸腔內科，台北市內湖區成功路二段 325 號

Coinfection with Pulmonary Tuberculosis and Cryptococcosis in an Immunocompetent Individual – A Case Report

Meng-Ju Tsai*,**, Chang-Ke Chu**

Coinfection with pulmonary tuberculosis and Cryptococcus species in an immunocompetent patient is uncommon, and sometimes the diagnosis is missed as the two infections share similar clinical manifestations. We encountered an 83-year-old male patient with the initial presentation of cough, sputum production and fever for 2 weeks. He denied any other remarkable history or systemic disease except chronic kidney disease, stage 2. Chest radiograph and computed tomography revealed a left upper lobe cavitary lesion with centrilobular nodules. Pulmonary tuberculosis and cryptococcal pneumonia were verified by positive sputum acid-fast stain and tuberculosis polymerase chain reaction, along with a positive serum cryptococcal antigen test. We also reviewed the literature and discussed the mechanism of coinfection with pulmonary tuberculosis and cryptococcosis. ***(Thorac Med 2014; 29: 105-111)***

Key words: coinfection, tuberculosis, cryptococcosis

Introduction

Cryptococcus species is ubiquitous worldwide and predominant in subtropical and tropical areas. It has been known as a leading cause of human morbidity and mortality, mostly among immunocompromised patients [1]. Cryptococcus species infecting healthy individuals has also been reported [2] -- pulmonary cryptococcosis is an example. People with pulmonary cryptococcosis are usually asymptomatic; however, the host lung immune system is impaired by the cryptococcal capsular component, which induces macrophage apoptosis, and the risk of tuberculosis (TB) is thereby increased [3-5]. *Mycobacterium tuberculosis* similarly affects the lung immune system by modulating cytokines [6-7]. The subtle interaction may help to explain the coinfection in some cases, including our patient in the following discussion.

*Department of Opthalmology, Taipei Tzu Chi Hospital, Buddhist Tzu Chi Medical Foundation, Taiwan R.O.C.
**Department of Chest Medicine and Critical Care Medicine, Cishan Hospital, Ministry of Health and Welfare, Kaohsiung, Taiwan, R.O.C.
Address reprint requests to: Dr. Chang-Ke Chu, Department of Critical Care Medicine and Chest Medicine, Cishan Hospital, Ministry of Health and Welfare, No. 60, Zhongxue Road, Cishan District, Kaohsiung City, 84247, Taiwan, R.O.C.

Case Report

An 83-year-old man presented with cough, sputum production and fever, along with general malaise and poor appetite for 2 weeks. He had chronic kidney disease, stage 2, but denied other systemic diseases. No remarkable past history or operation was documented. He did not smoke, drink or take any medicine such as corticosteroid long term. He denied any travel history or contact with birds. Also, there was no known exposure to TB. On examination, body temperature was 37.9°C; pulse, 96 beats per minute; respiratory rate, 21 breaths per minute; and blood pressure, 101/56 mmHg. Chest auscultation revealed bilateral coarse breathing sounds. The hemogram at admission showed a white blood cell (WBC) count of 8300/uL, with neutrophils at 90.1%. Biochemical tests for kidney function showed blood urea nitrogen (BUN) 112 mg/dL and creatinine (Cr) 3.4 mg/dL.

The chest radiograph initially revealed increased infiltrates with cavitation in the left upper lung field (Figure 1). Broad-spectrum antibiotics with piperacillin/tazobactam (2.25 gm every 8 hours) were empirically prescribed for pneumonia, but coexistence of pulmonary TB could not be excluded. One week later, both the sputum acid-fast stain and TB-polymerase chain reaction were positive, which confirmed the diagnosis of pulmonary TB. High-resolution computed tomography of the lung revealed centri-lobular nodules and well-defined cavitation in the left upper lobe (Figures 2, 3) and right middle lobe (Figure 4). Anti-TB agents were thus added, with rifampicin (RIF) (450 mg once daily), isoniazid (INH) (300 mg once daily), ethambutol (EMB) (800 mg 3 times weekly) and pyrazinamide (PZA) (1000 mg 3 times weekly). However, intermittent spiking fever persisted for about 1 week after anti-TB drug administration. Because of a highly suspected nosocomial infection, the antibiotics were upgraded to cefepime (2.0 gm every 12 hours). Later, the serum cryptococcal antigen test taken at admission was found to be 1:8(+).

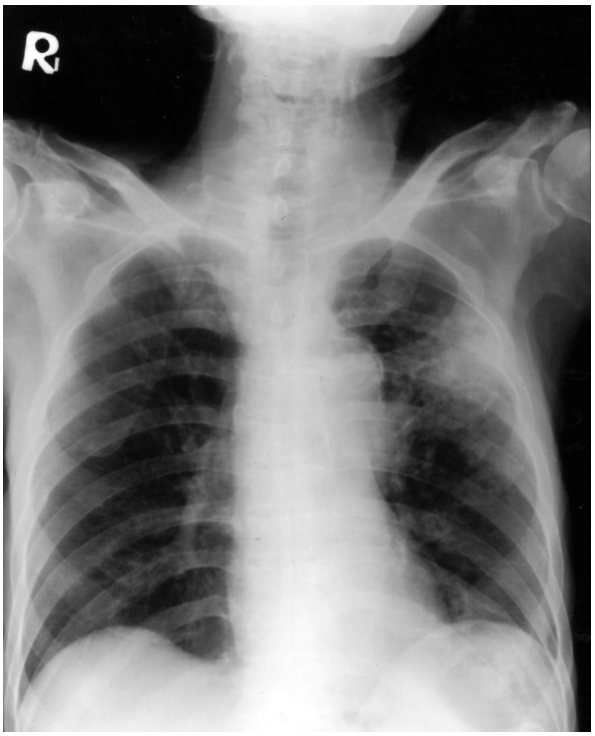

Fig. 1. Cavitation with patchy infiltrates in the left upper lobe.

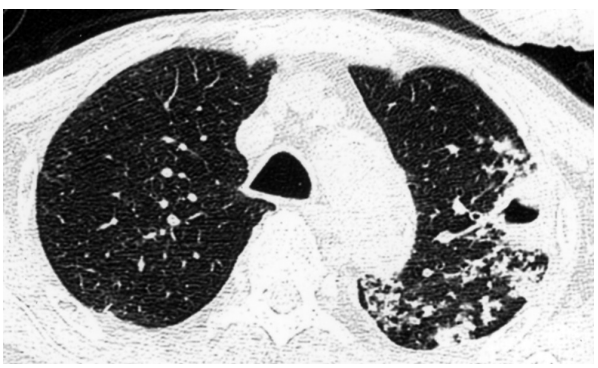

Fig. 2. Centri-lobular nodules with 1 well-defined cavitation, about 1.2 cm x 0.8 cm in size, noted in the left upper lobe.

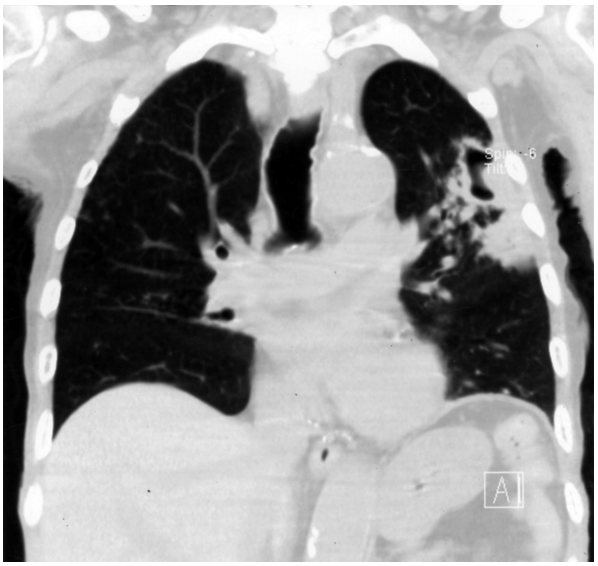

Fig. 3. Coronal view of the cavitary lesion mentioned in Figure 2.

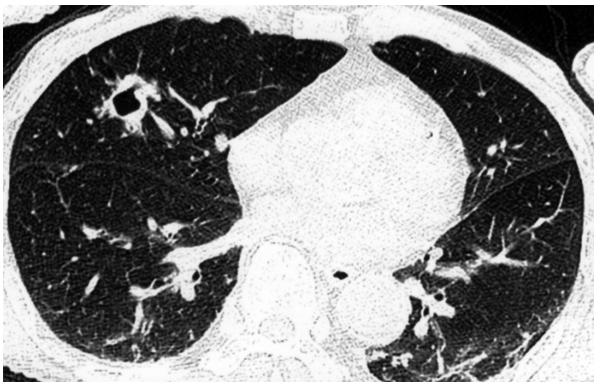

Fig. 4. One well-defined cavitation at the right middle lobe.

We therefore initiated anti-fungal agents with fluconazole (200 mg once daily). Lumbar puncture was performed to exclude cryptococcal meningitis. The patient's cerebrospinal fluid (CSF) analysis showed a WBC count of 3/μL, with polymorphonuclear leukocytes (PMN) at 33% and an absence of lymphocytes. The CSF glucose level was 71 mg/dL and protein level was 42 mg/dL. Blood fungus culture yielded no growth. HIV serology was negative. The fever subsided after 2 days of anti-fungal and anti-TB

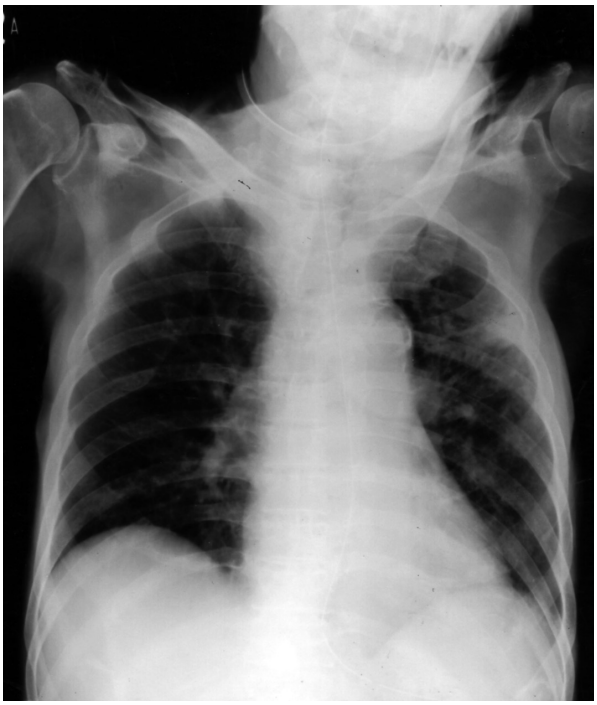

Fig. 5. Resolution of the cavitation at the left upper lobe after treatment.

treatment. We also discontinued the antibiotics due to a lack of evidence of bacterial growth. The sputum acid-fast stain after 2 weeks of anti-TB medication showed a negative result. Chest radiograph also showed resolution of the cavitation and infiltrates (Figure 5). The patient tolerated the medication well and did not develop hepatotoxicity or any other side effects. (The first 4 weeks of treatment are summarized in Figure 6.) After 8 weeks in the hospital, he was discharged and continued the anti-TB regimen with fluconazole medication in the outpatient department.

Discussion

Cryptococcus species is ubiquitous worldwide and is acquired primarily by inhaling spores of Cryptococcus in the environment [1].

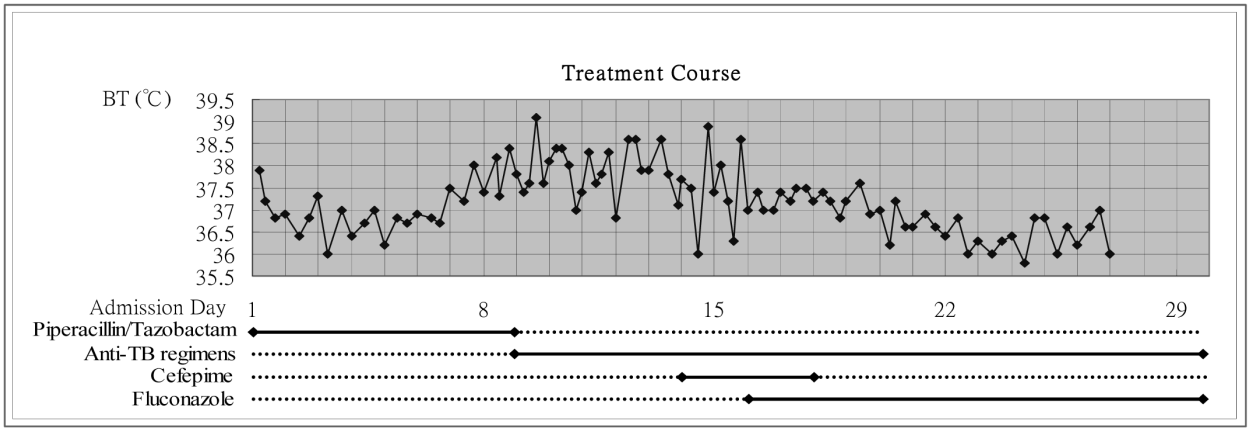

Fig. 6. Brief summary of the first 4 weeks of treatment.

Following inhalation, it may trigger the human immune system, causing focal pneumonitis, or to a more severe extent, disseminate to the central nervous system causing meningitis or to other parts of human body. The patient's immune status plays a key role in determining clinical outcomes. Immunocompetent individuals may be asymptomatic or present with non-specific symptoms and signs like cough, sputum production, dyspnea, hemoptysis, and fever; however, in immunocompromised patients, Cryptococcus infection may be fatal [2]. Cryptococcus species are encapsulated yeasts and can be subclassified according to different serotypes [4]. Immunocompetent individuals are predisposed to *C. gattii* despite the fact that *C. gattii* infects a certain number of patients with immune disorders; immunocompromised patients are more likely to acquire *C. neoformans* species. Cryptococcus species exerts its virulence via capsular polysaccharide [3].

Cryptococcal capsular polysaccharide mainly consists of galactoxylomannan (GalXM) and glucuronoxylomannan (GXM), which exert various immunomodulatory effects on human immune responses. Studies have shown that capsular polysaccharide induces production of the anti-inflammatory cytokine interleukin-10 (IL-10), and transforming growth factor-β (TGF-β), which may down-regulate the lung immune system by impairing T helper type 1 (Th1) cells and inhibiting interferon-γ (IFN-γ)-related activities responsible for killing tubercle bacilli [3]. Some reports have also demonstrated that GXM promotes macrophage nitric oxide (NO) induction in rat models via a variety of receptors and intracellular kinase activation, causing macrophage apoptosis [4]. Macrophage apoptosis promoted by inducing Fas/FasL expression on macrophages was also shown in another study [5]. The importance of macrophages in the defense against TB has been illustrated as well. Inhibition of Mycobacterium bacilli by macrophages through various mechanisms has been well described [6-7,11]. Phagocytosis of bacilli by alveolar macrophages is viewed as the initial step in the host-pathogen relationship that determines the outcome of infection [11]. All of the mechanisms mentioned above result in impairment of host immune systems and illu-

minate how TB more likely affects human bodies.

On the other hand, TB also has a negative impact on the immune system of the lung. It is well-known that alveolar macrophages phagocytose and clear off tubercle bacilli by NO production via expression of NO synthase, and that the Th1 type response is important in countering TB. However, TB, to a significant extent, causes more IL-10 production and elevated co-expression of TGF-β and its receptors than other lung diseases in TB patients, which leads to T cell anergy in response to Mycobacterium pathogens, and antagonizes macrophage IFN-γ-related activities that are thought to be important defense mechanisms [6-7].

Since macrophages play a crucial role in the defense against both TB and cryptococcosis, macrophage apoptosis is a detriment to the host immune system, which is necessary to eliminate the virulence of these pathogens. By using this biomolecular point of view to investigate how TB and Cryptococccus affect the host immune system, we can infer that each of them contributes partly to host immune impairment in a similar way, which also leads to susceptibility to other infections and overt disease.

In this report, we discussed the case of an immunocompetent male patient with pulmonary TB and cryptococcal infection. However, it was impossible for us to know whether TB preceded cryptococcal pneumonia or vice versa. Though we did not present a Cryptococcus serotype in this case, most immunocompetent individuals tend to be infected with *C. gattii*, as we discussed earlier. Risk factors for *C. gattii* also include age over 50 (usually 70-79 years) and male gender [8]. Based on IDSA guidelines for cryptococcal pneumonia without central nervous system involvement, this case was treated with fluconazole 400 mg once daily orally for 6 to 12 months [9]. Anti-TB treatment began with a combination of INH, RIF, EMB, and PZA for 2 months, followed by 4 months of a continuation phase with INH and RIF, according to the MMWR protocol [10].

Conclusion

Coinfection with pulmonary TB and Cryptococcus species is rare in immunocompetent patients. Either infection can suppress the lung immune system, which promotes susceptibility to infection by the other. We should always consider more than 1 infection, especially in those under treatment for a certain pathogen yet still with an inadequate response.

References

1. Chen YC, Chang SC, Shih CC, *et al*. Clinical features and in vitro susceptibilities of two varieties of *Cryptococcus neoformans* in Taiwan. Diagn Microbiol Infect Dis 2000; 36: 175-83.
2. Chu HQ, Li HP, He GJ. Analysis of 23 cases of pulmonary cryptococcosis. Chin Med J 2004; 117(9): 1425-7.
3. Ellerbroek PM, Walenkamp AM, Hoepelman AI, *et al*. Effects of the capsular polysaccharides of *Cryptococcus neoformans* on phagocyte migration and inflammatory mediators. Curr Med Chem 2004; 11: 253-66.
4. Chiapello LS, Baronetti JL, Garro AP, *et al*. *Cryptococcus neoformans* glucuronoxylomannan induces macrophage apoptosis mediated by nitric oxide in a caspase-independent pathway. Int Immunol 2008; 20: 1527-41.
5. Villena SN, Pinheiro RO, Pinheiro CS, *et al*. Capsular polysaccharides galactoxylomannan and glucuronoxylomannan from *Cryptococcus neoformans* induce macrophage apoptosis mediated by Fas ligand. Cell Microbiol 2008; 10: 1274-85.
6. Almeida AS, Lago PM, Boechat N, *et al*. Tuberculosis is associated with a down-modulatory lung immune response that impairs Th1-type immunity. J Immunol 2009;

183: 718-31.

7. Bonecini-Almeida MG, Ho JL, Boe´chat NL, *et al*. Down-modulation of lung immune responses by interleukin-10 and transforming growth factor (TGF-β) and analysis of TGF-β receptors I and II in active tuberculosis, Infect Immun 2004; 72: 2628-34.
8. MacDougall L, Fyfe M, Romney M, *et al*. Risk factors for *Cryptococcus gattii* infection, British Columbia, Canada. Emerg Infect Dis 2011; 17: 193-9.
9. Perfect JR, Dismukes WE, Dromer F, *et al*. Clinical practice guidelines for the management of cryptococcal disease: 2010 update by the Infectious Diseases Society of America. Clin Infect Dis 2010; 50(3): 291-322.
10. Centers for Disease Control and Prevention. Treatment of Tuberculosis, American Thoracic Society, CDC, and Infectious Diseases Society of America. MMWR 2003; 52(No. RR-11): 3,6,20-25.
11. Raja A. Immunology of tuberculosis. Indian J Med Res 2004; 120(4): 213-32.

免疫健全的狀態下同時感染肺結核與隱球菌－病例報告

蔡孟儒 *,** 曲長科 **

對一位免疫健全的病人而言，同時感染肺結核與隱球菌兩者是很罕見的，臨床上因兩者表現相似而更不易做出正確診斷。我們探討一位八十三歲男性病人初期表現為咳嗽、痰多與發燒兩週，除了慢性腎病第二期外，並沒有其他過去病史。胸部 X 光與電腦斷層檢查顯示左側上肺葉開洞與小葉中心結節病灶，痰液抗酸性染色與結合分枝桿菌聚合酶連鎖反應檢驗皆顯示陽性，血清隱球菌抗原測試亦為陽性，因而確診肺結核與肺部隱球菌感染。我們藉由回顧文獻，探討兩者對於肺部免疫機制的交互影響。*(胸腔醫學 **2014; 29: 105-111**)*

關鍵詞：肺結核，隱球菌，免疫健全

* 佛教慈濟醫療財團法人台北慈濟醫院　眼科部，** 衛生福利部旗山醫院　胸腔內科暨重症加護病房
索取抽印本請聯絡：曲長科醫師，衛生福利部旗山醫院　胸腔內科暨重症加護病房，高雄市旗山區大德里中學路 60 號

Pulmonary Sequestration Complicated with *Mycobacterium abscessus* Infection: Report of a Case

Jheng-Wei Liou*, Shih-Lung Cheng*,**

Pulmonary sequestration is a congenital abnormality of lung tissues and receives its blood supply from systemic arteries. Intralobar pulmonary sequestration has its own pleural covering. The typical presentation of pulmonary sequestration is recurrent infection; however, the organisms causing sequestrated lung infections have seldom been reported. We report the case of a 27-year-old female patient who presented with chronic cough for months. Pulmonary sequestration with secondary infection was suspected based on the symptoms and typical radiographic manifestations. Chest computed tomography angiography confirmed the diagnosis. The patient underwent a right lower lobe lobectomy by video-assisted thoracoscopic surgery. A surgical infection developed after the operation, and subsequent cultures of wound pus and sequestrated lung tissue grew *Mycobacterium abscessus*. The patient recovered from the inflammatory process after debridement and antibiotic therapy with clarithromycin and levofloxacin for 6 months. ***(Thorac Med 2014; 29: 112-117)***

Key words: pulmonary sequestration, *Mycobacterium abscessus*

Introduction

Pulmonary sequestration is a segment of the lung that lacks normal communication with the tracheobronchial tree and derives its arterial blood supply from systemic circulation. When a pulmonary sequestration communicates with the bronchial tree, it is often complicated with infection. Patients often present with signs of recurrent pneumonia. Despite the high frequency of infections, there is a lack of data regarding the specific infecting organisms [1]. A sequestrated lung infected with *Mycobacterium abscessus* (*M. abscessus*) is rare and has been described in only 1 previous case report [2]. Herein, we report a case of intralobar pulmonary sequestration associated with an *M. abscessus* infection.

Case Report

A 27-year-old woman visited our clinic due to dry cough and exertional dyspnea for months. She was previously healthy and reported no history of smoking or drinking alcohol. Other symptoms included nasal congestion and

*Internal Medicine, Far Eastern Memorial Hospital, New Taipei City, Taiwan; **Department of Chemical Engineering and Materials Science, Yuan-Ze University, Taoyuan Country, Taiwan
Address reprint requests to: Dr. Shih-Lung Cheng, Department of Internal Medicine, Far Eastern Memorial Hospital, No. 21, Nanya S Rd. Banciao, New Taipei City, Taiwan

rhinorrhea. She denied hemoptysis, fever, chills, night sweats, anorexia, and weight loss. A chest X-ray (Figure 1) showed consolidation at the right lower lung field. Chest computed tomography (CT) showed consolidation at the right lower lung, with localized emphysematous and cystic change in the adjacent lung parenchyma.

On admission, her blood pressure was 108/74 mmHg, pulse rate 106 beats per minute, respiratory rate 20 breaths per minute, and temperature 37.7°C. Auscultation of bilateral lung fields revealed clear breathing sounds, and no cyanosis or digital clubbing was noted. Laboratory studies disclosed a serum white blood cell count of $5.58\times10^3/\mu l$ (neutophils 69.3%, lymphocytes 13.6%), and negative for serum cryptococcus antigen. Sputum acid-fast stain and mycobacterial cultures were negative. Chest

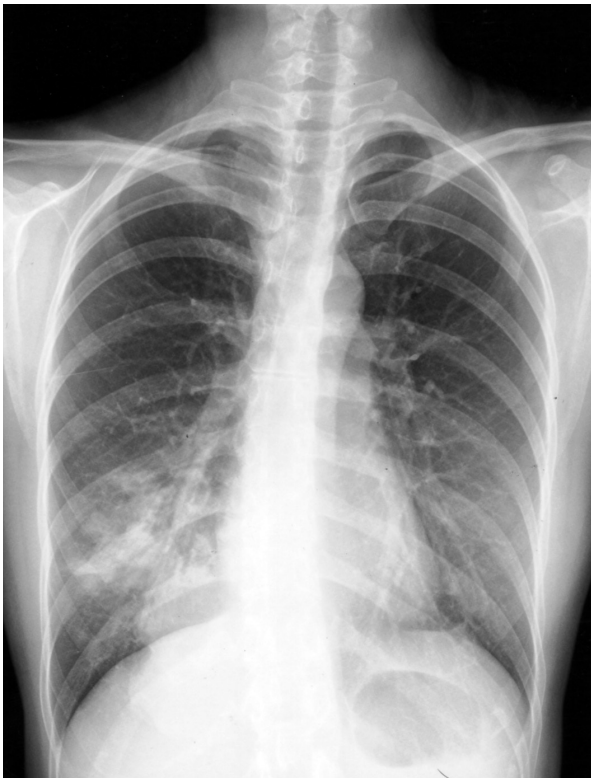

Fig. 1. Consolidation patch at the right lower lung field

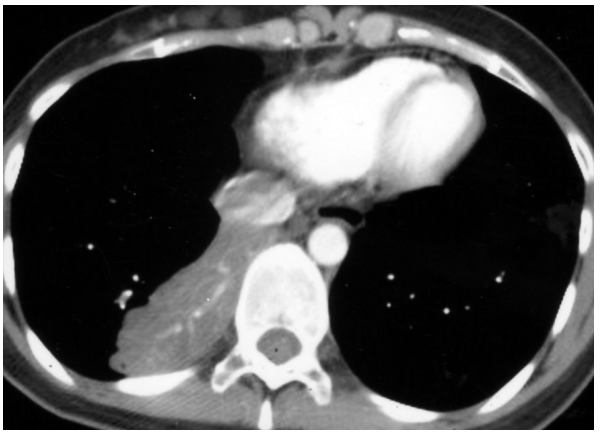

Fig. 2A. Consolidation in the posterior basal segment of the right lower chest and azygoesophageal recess.

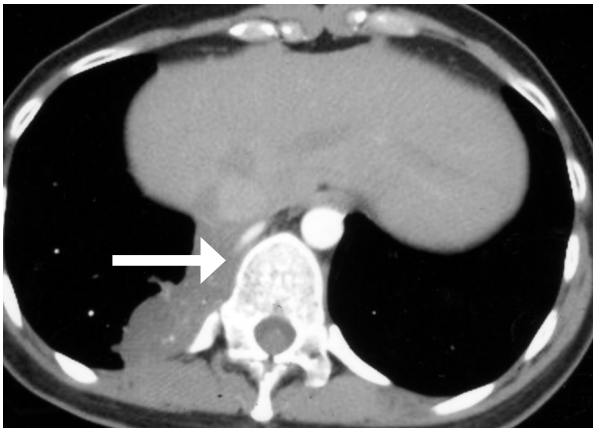

Fig. 2B. Engorged feeding artery (white arrow) derived from the abdominal aorta (sharing a common trunk with the celiac trunk)

CT angiography (Figures 2A and 2B) showed consolidation in the right lower chest and azygoesophageal recess, with an engorged feeding artery derived from the abdominal aorta (sharing a common trunk with the celiac trunk), and draining into the right pulmonary vein. Intralobar pulmonary sequestration was suspected. Lobectomy of the right lower lobe using video-assisted thoracoscopic surgery was performed and a 6×6 cm consolidation with a large amount of yellowish sputum within the lesion was resected. One feeding artery arising from the de-

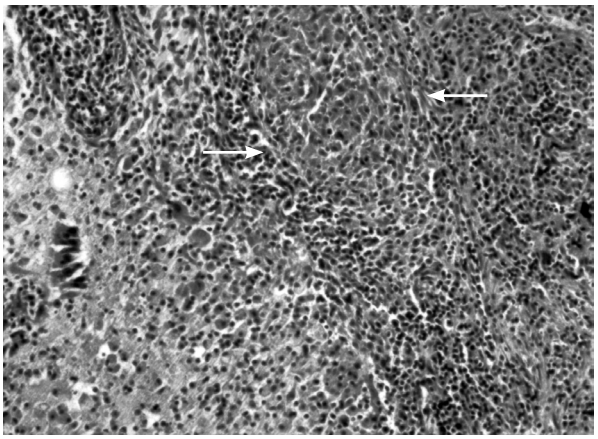

Fig. 3A. Pulmonary sequestration. Photomicrograph (original magnification, ×200; H-E stain) of resected pulmonary tissue showed mixed acute and chronic inflammatory infiltration. Granulomatous inflammation was present (arrows).

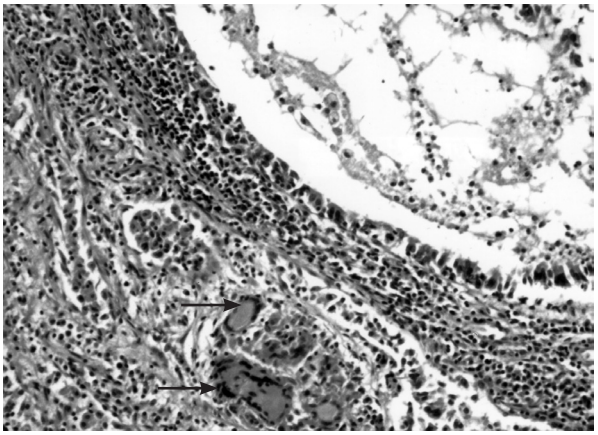

Fig. 3B. Pulmonary sequestration. Photomicrograph (original magnification, ×200; H-E stain) of resected pulmonary tissue showed infiltration of multiple inflammatory cells and multinucleated giant cells (small arrows). Some bronchioles were filled with mucoid secretion.

scending aorta was visualized during the operation. Pathology (Figures 3A and 3B) showed an abscess with mixed acute and chronic inflammatory infiltration. Granulomatous inflammation and multinucleated giant cells were present, along with a dilated bronchus and bronchiole, inflammatory infiltration, and mucoid secretion. A subsequent tissue culture grew *M. abscessus*.

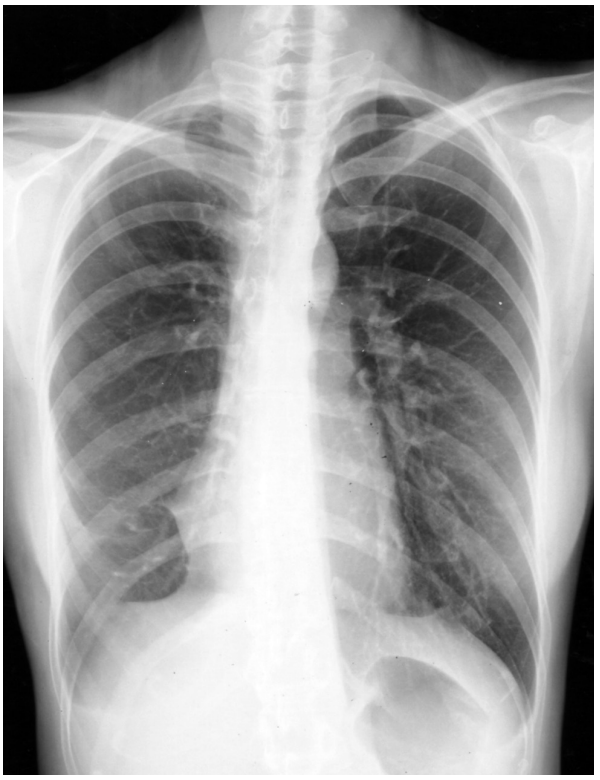

Fig. 4. Six months post-operation, no recurrence of right lower lobe consolidation was seen

Wound festering with a purulent discharge was noted after the operation, and improved with debridement. The patient was discharged in a stable condition and followed up at our clinic. Pus culture of the infected site also grew *M. abscessus*. Clarithromycin and levofloxacin were then prescribed for 6 months. A chest X-ray after 6 months (Figure 4) showed no recurrence of right lower lobe consolidation, and that the wound had recovered well.

Discussion

Pulmonary sequestration is a segment of lung that lacks normal communication with the tracheobronchial tree and derives its arterial blood supply from systemic circulation. Pulmonary sequestration is classified into intralobar

and extralobar types, depending on whether or not the abnormal lung tissue possesses its own pleural covering. Extralobar pulmonary sequestrations are masses of lung parenchyma that have a distinct pleural covering maintaining complete anatomical separation of the mass from adjacent normal lung tissue. In contrast, intralobar pulmonary sequestrations are masses of lung parenchyma that are contiguous with the adjacent normal lung [3]. The pathogenesis of pulmonary sequestration involves a part of the lung tissue with an aberrant arterial supply during the embryonic period developing into a separate lesion with no respiratory function [4].

The typical manifestation of sequestration on chest radiography is focal opacities in the posterior, inferior, and medial aspect of either hemithorax (more commonly on the left side). The opacity of sequestration on chest radiography is non-specific and can be homogenously opaque, an ill-defined margin, a cystic lesion or contain an air-fluid level. The radiographic appearance may also mimic a mass lesion, and thus, it is often misdiagnosed as pneumonia, lung abscess, and lung cancer or mediastinal tumor. However, clinical conditions often suggest a diagnosis based on the typical location of the lesion and a past history of recurrent infection at the same location. The diagnosis of pulmonary sequestration should include the anomalous systemic arterial blood supply, which can be seen on CT angiography, magnetic resonance angiography and digital subtraction angiography [4]. The treatment for symptomatic pulmonary sequestration is surgical excision, which often requires a lobectomy [5]. Surgical treatment for asymptomatic pulmonary sequestration is still controversial; however, some clinicians advocate surgery for asymptomatic patients due to the risk of infection and to exclude other pathologies [6].

A sequestrated lung is often complicated with infection, especially when it communicates with normal lung tissue. A few reports have identified the infectious organisms as Staphylococcus, Pseudomonas, Aspergillus, *M. tuberculosis* and nontuberculous Mycobacterium [2,7-9]. However, pulmonary sequestration infected with *M. abscessus* is rare. According to the literature review, ours is the second case of pulmonary sequestration infected with *M. abscessus* [2]. Combination antibiotic therapy including a macrolide and 1 or more parenteral agents is suggested for the treatment of *M. abscessus* lung disease [10]. However, no definite combined regimen, even based on *in vitro* susceptibilities, can provide a cure for *M. abscessus* lung disease. In the current case, surgical resection did cure the pulmonary sequestration. In theory, surgical resection also removes the infected lung. A few case reports have discussed the need to use antibiotics after surgical resection of a sequestrated lung infected with nontuberculous Mycobacterium. In 1 report, surgical resection was performed without antimycobacterial agents for a sequestrated lung infected with *M. kansasii* [1]. In another case report, a combined antibiotic regimen was prescribed after surgical resection of a sequestrated lung infected with *M. abscessus* [2]. In our case, clarithromycin and levofloxacin were prescribed for a total of 6 months due to wound infection. The patient's wound recovered well and follow-up chest X-ray showed no recurrence of infection.

In conclusion, pulmonary sequestration complicated with *M. abscessus* infection is rare. The treatment involves resection whenever possible. The benefit of antibiotics treatment after resection of the infected sequestrated lung re-

mains uncertain.

References

1. Lin SH, Lee LN, Chang YL, *et al*. Infected pulmonary sequestration caused by *Mycobacterium kansasii*. Thorax 2005; 60: 355.
2. Koh WJ, Hong G, Kim K, *et al*. Pulmonary sequestration infected with nontuberculous mycobacteria: a report of two cases and literature review. Asian Pac J Trop Med 2012; 5: 917-9.
3. Corbett HJ, Humphrey GME. Pulmonary sequestration. Paediatric respiratory reviews 2004; 5: 59-68.
4. Wei Y, Li F. Pulmonary sequestration: a retrospective analysis of 2625 cases in China. Eur J Cardiothorac Surg 2011; 40: e39-42.
5. Halkic N, Cuénoud PF, Corthésy ME, *et al*. Pulmonary sequestration: a review of 26 cases. Eur J Cardiothorac Surg 1998; 14: 127-33.
6. Cho MJ, Kim DY, Kim SC, *et al*. Embolization versus surgical resection of pulmonary sequestration: clinical experiences with a thoracoscopic approach. J Pediatr Surg 2012; 47: 2228-33.
7. Collin PP, Desjardins JG, Khan AH. Pulmonary sequestration. J Pediatr Surg 1987; 22; 750-3.
8. Morikawa H, Tanaka T, Hamaji M, *et al*. A case of aspergillosis associated with intralobar pulmonary sequestration. Asian Cardiovasc Thorac Ann 2011; 19: 66-8.
9. Elia S, Alifano M, Gentile M, *et al*. Infection with *Mycobacterium tuberculosis* complicating a pulmonary sequestration. Ann Thorac Surg 1998; 66: 566-7.
10. Griffith DE, Aksamit T, Brown-Elliott BA, *et al*. An official ATS/IDSA statement: diagnosis, treatment, and prevention of nontuberculous mycobacterial disease. Am J Respir Crit Care Med 2007; 175: 367-461.

肺隔離症併發膿腫分枝桿菌感染：病例報告

劉正偉 * 鄭世隆 *,**

肺隔離症是一種先天性異常的肺組織，其接收主動脈的血液供應。葉內型肺隔離症有其自己的肋膜覆蓋。肺隔離症的典型表現是反覆的肺感染。然而感染肺隔離症的菌種卻很少被報導。我們報告一位 27 歲的女性病人因為慢性咳嗽數月而來求診。我們根據其症狀與典型的 X 線表現而懷疑肺隔離症繼發感染。胸部電腦斷層造影證實診斷。該病人藉由電視胸腔鏡手術（VATS）接受右下肺葉切除術。此病人手術後發生傷口感染。傷口膿液和肺組織的培養報告皆顯示膿腫分枝桿菌。病人的傷口清創後合併抗生素治療（clarithromycin and levofloxacin）共六個月。之後，復原狀況良好，無復發現象。*(胸腔醫學 **2014; 29: 112-117**)*

關鍵詞：肺隔離症，膿腫分枝桿菌

* 亞東紀念醫院　內科部　胸腔內科，** 元智大學　化學工程及材料科學學系
索取抽印本請聯絡：鄭世隆醫師，亞東紀念醫院　內科部　胸腔內科，新北市板橋區南雅南路二段 21 號

Successful Treatment of Lipoid Pneumonia with Steroid – A Case Report and Literature Review

Huai-Lei Juan*, Chih-Jen Yang*,***,****, Hsin-Ling Yin**, Tung-Heng Wang*,*****, Jhi-Jhu Hwang*,*****, Ming-Shyan Huang*,****

Lipoid pneumonia is an uncommon disease that results from pulmonary accumulation of a fat-like component. The diagnosis is based on clinical history, radiologic presentation and bronchoalveolar lavage (BAL) sample analysis. We report the case of a 46-year-old male who presented with cough, fever and pleuritic chest pain after diesel oil aspiration. Chest radiograph on admission revealed consolidation in the right lower lung field; an antibiotic was administered to treat aspiration pneumonia. Bronchoscopy revealed some oily, transparent, yellowish fluid in the right lower bronchus, but culture and cytology of BAL fluid showed negative results. The follow-up chest radiograph revealed no obvious improvement after antibiotic treatment. Chest computed tomography (CT) revealed consolidation in the right middle lobe with heterogeneous density, and CT-guided biopsy revealed necrotizing inflammation. A follow-up bronchoscopy showed mucosal inflammation. Steroid was administered to treat the lipoid pneumonia and inflammation, and obvious improvement of the clinical symptoms and radiologic manifestations was seen. No specific adverse effect or complication was noted during therapy. In patients with lipoid pneumonia, careful history-taking and diagnosis are important. Steroid is effective for these patients. ***(Thorac Med 2014; 29: 118-125)***

Key words: lipoid pneumonia, pneumonia, bronchoscopy

Introduction

Lipoid pneumonia is an uncommon disease that results from pulmonary accumulation of a fat-like component. The diagnosis is based on clinical history, radiologic presentation and bronchoalveolar lavage (BAL) sample analysis.

Case Presentation

A 46-year-old male truck driver with an unremarkable medical history aspirated a mouthful of diesel oil when he tried to refuel his truck. Cough with watery sputum, fever, chills, cold sweating, fatigue, myalgia, right pleuritic chest

*Division of Pulmonary and Critical Care Medicine, Department of Internal Medicine; **Department of Pathology, Kaohsiung Medical University Hospital; ***Department of Internal Medicine, Kaohsiung Municipal Ta-Tung Hospital; ****Department of Internal Medicine, School of Medicine, College of Medicine; *****Department of Respiratory Therapy, College of Medicine, Kaohsiung Medical University, Kaohsiung, Taiwan
Address reprint requests to: Dr. Ming-Shyan Huang, Division of Pulmonary and Critical Care Medicine, Department of Internal Medicine, Kaohsiung Medical University Hospital, Kaohsiung Medical University, No. 100, Tzyou 1st Road, Kaohsiung 807, Taiwan

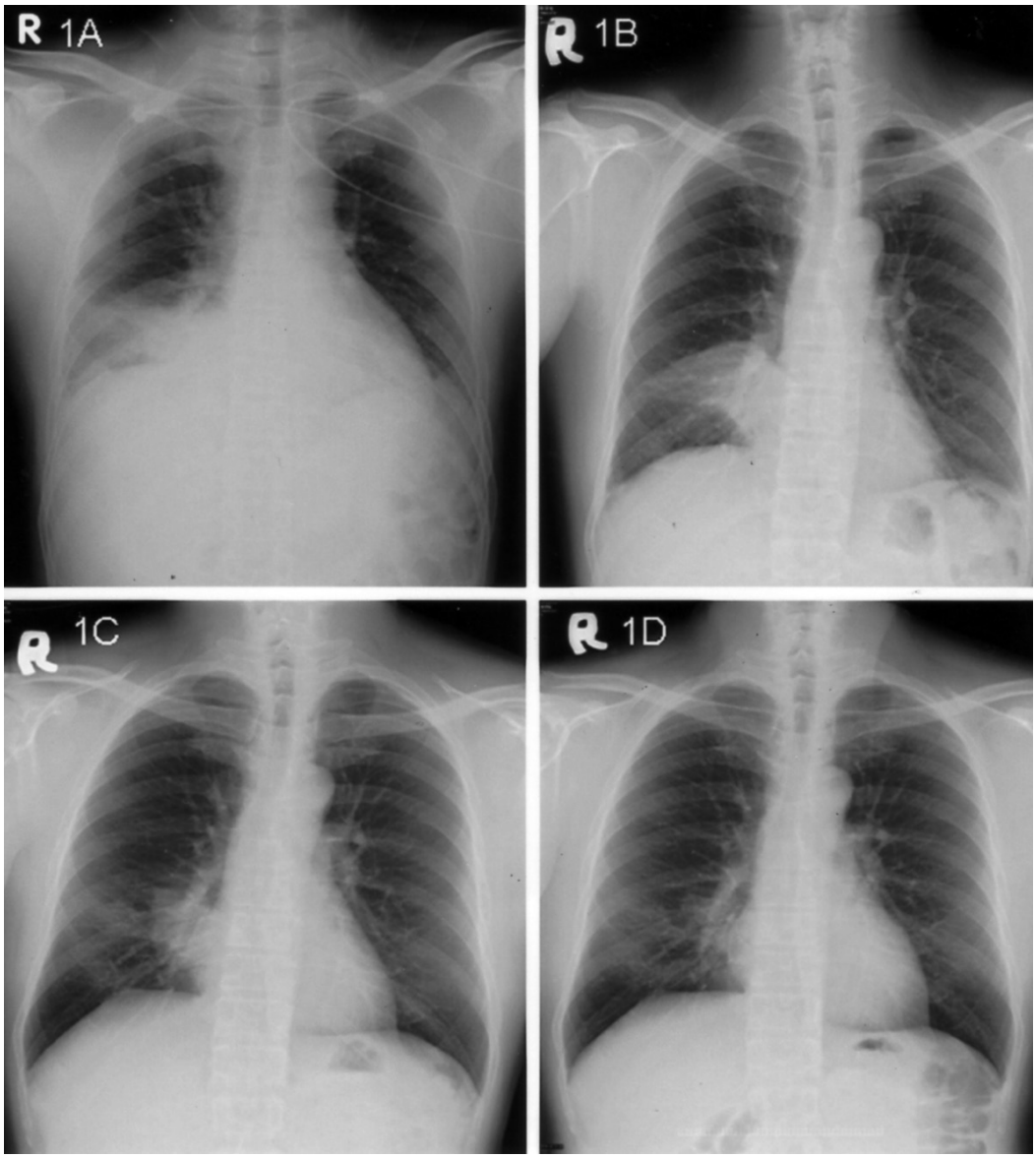

Fig. 1. The chest radiograph taken on presentation (A) showed consolidation in the right lower lung field. The follow-up chest radiograph taken 2 weeks after treatment (B) and 4 weeks after treatment (C) showed gradual resolution of the pneumonia patch. The follow-up exam 9 months later (D) revealed nearly total resolution.

pain and exertional dyspnea developed within 1 day. He then visited the emergency department, where fever up to 38°C without tachypnea or tachycardia was noted. Laboratory exams revealed leukocytosis (23400/μL) with a left shift (7.5% band forms) and an elevated C-reactive protein level. Chest radiograph revealed increased opacity in the right lower lung field (Figure 1). An empirical antibiotic was given, and the patient was admitted for further treatment of probable aspiration pneumonia.

After admission, the antibiotic treatment was maintained. Bronchoscopy was arranged due to the oil aspiration incident, and revealed

some oily, transparent, yellowish fluid in the right lower bronchus, consistent with diesel oil accumulation (Figure 2). Further analysis of the bronchoalveolar lavage (BAL) fluid revealed no specific pathogen or malignant cell. The cell differential count of the BAL fluid was not available as it is not examined routinely. Since the opacity in the right lower lung field persisted after 3 days of antibiotic treatment, computed tomography (CT) of the chest was arranged for further assessment, and revealed consolidation of the right middle lobe with heterogeneous density and right pleural effusion with passive atelectasis of the right lower lobe (Figure 3). After continuing antibiotic treatment for 7 more days for a suspected lung abscess without liquification, the fever, dyspnea and pleuritic chest pain subsided. However, the chest radiograph revealed persistent consolidation in the right lower lung field, so CT-guided biopsy was done to exclude malignancy or other parenchymal lesion. The pathological examination of the specimens showed necrotizing inflammation (Figure 4). A follow-up bronchoscopy to further assess the persistent lesion in the right lower lung field showed mild mucosal inflammation without an endobronchial mass lesion or yellowish fluid. On day 12 of antibiotic treatment, steroid (prednisolone 10 mg 3 times per day) was added to treat the inflammation related to the lipoid pneumonia; his symptoms, including cough, dyspnea and chest pain, improved

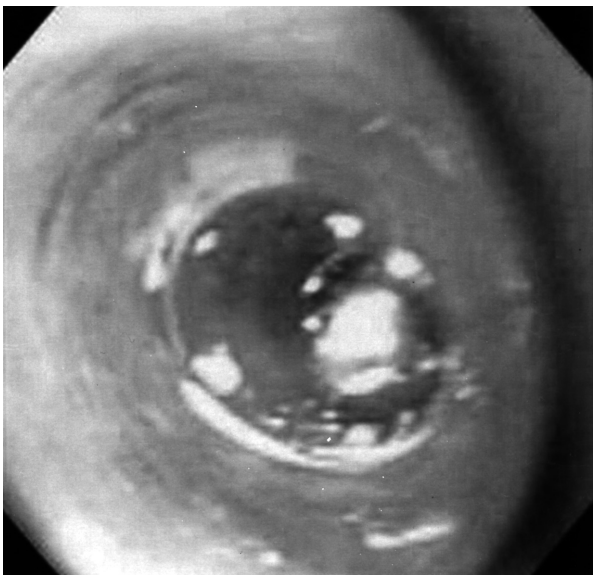

Fig. 2. Bronchoscopy revealed some yellowish fluid in the right middle lobe bronchus.

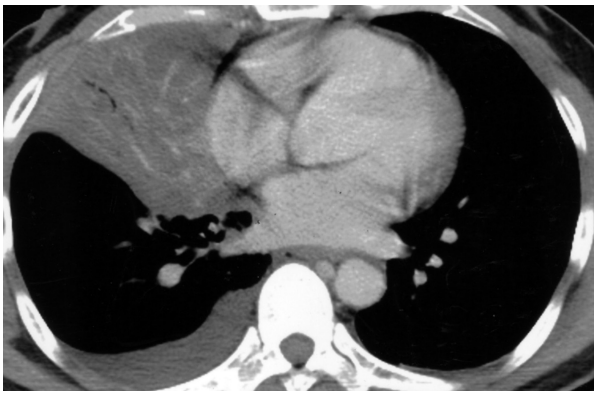

Fig. 3. Computed tomography of the chest showed marked consolidation of the right middle lobe with heterogeneous density and right pleural effusion with passive atelectasis of the right lower lobe.

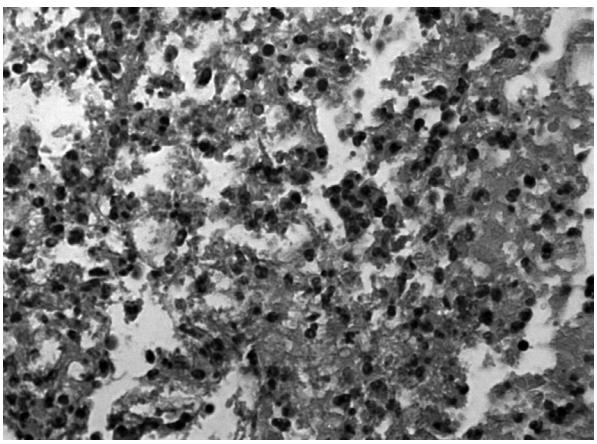

Fig. 4. CT-guided biopsy revealed necrotic debris with acute inflammatory cell infiltrates. (H&E stain, original magnification of 40x obj)

gradually thereafter, with the chest radiograph confirming the improved course. Antibiotic was administered for 14 days and the prednisolone dose was tapered gradually and discontinued 3 months later. He had a complete recovery.

Discussion

Lipoid pneumonia is an uncommon disease that results from the pulmonary accumulation of fat-like compounds of animal, vegetable or mineral origin [1]. It has been reported predominantly in children, but is also found in healthy people, and is sometimes related to occupational exposure [2-3]. Lipoid pneumonia can be classified into endogenous and exogenous forms based on the source of the accumulated fat; fat aspiration or inhalation is a central causative factor of exogenous lipoid pneumonia. In endogenous lipoid pneumonia, intra-alveolar lipid accumulation occurs as a result of obstruction, chronic lung infection or lipid storage disorder, and the diagnosis is made on demonstrating lipid-laden macrophages. The exogenous form can be classified into acute and chronic types based on the course [4]. Acute exogenous lipoid pneumonia, which is caused by an episode of aspiration of a large quantity of a petroleum-based product, is uncommon. Chronic exogenous lipoid pneumonia is more common and is related to repeated aspiration of oil or fatty substances. The clinical symptoms of acute exogenous lipoid pneumonia may imitate those of infectious pneumonia with fever, and the chronic form usually presents with dyspnea and cough. The radiologic presentations of acute and chronic exogenous lipoid pneumonia are similar.

The clinical symptoms are nonspecific and vary, depending on the patient's age, duration of oil intake, and the amount and quality of oil aspirated [1,5]. The presentation of acute exogenous lipoid pneumonia may be similar to that of infectious pneumonia, and typically manifests clinically as cough, dyspnea and low-grade fever, sometimes accompanied with chest pain, hemoptysis or weight loss. Extra-thoracic symptoms, such as vomiting, epigastralgia, dysphagia, vertigo and fainting, are occasionally reported in the literature [6]. Our patient presented with cough, dyspnea, fever and chest pain, which are typical symptoms of acute exogenous lipoid pneumonia.

The diagnosis of exogenous lipoid pneumonia is based on a history of exposure to oil, radiological findings and the presence of lipid-laden macrophages in sputum or BAL fluid [4,7-8]. The correct diagnosis is easily missed because the clinical symptoms imitate those of infectious pneumonia, and the history of oil aspiration is usually overlooked. The diagnosis in our case was made early because of the careful history-taking.

Acute exogenous lipoid pneumonia is usually manifested on chest radoiograph within 24 hours after the episode of aspiration or inhalation. On the chest radiograph, it typically presents as ground-glass opacities or consolidations involving bilateral lower lobes and the right middle lobe [4,8-9]. High-resolution CT is the imaging modality of choice, characteristically presenting consolidations with areas of fat attenuation [7,10-11]. The radiologic manifestations of lipoid pneumonia usually resolve within 2 weeks, but may persist for 8 months [8,12]. In our case, the chest radiograph revealed consolidation in the right lower lung field that developed within 24 hours of the aspiration episode and resolved within a few weeks, consistent with the typical radiologic evolution

of lipoid pneumonia.

Bronchoscopy with BAL is helpful in establishing the diagnosis [7-8]. The BAL fluid is typically whitish or turbid, with fat globules on the fluid surface. The presence of extracellular oily droplets and lipid-laden macrophages is more specific for exogenous lipoid pneumonia [13]. More than 1.0 ml of BAL fluid should be collected, and no fixative is added. The BAL fluid is centrifuged, and analyzed with special stain. An Oil-Red-O or Sudan black-stained slide of the pooled sample is examined microscopically and macrophages are graded by the amount of lipid in the cytoplasm of each cell to obtain the lipid-laden macrophages index [14-15]. However, the diagnostic value of lipid-laden macrophage identification is still questioned by some authors [15-16]. In our case, although the BAL cytology and lung biopsy pathology revealed negative and non-specific findings respectively, the diagnosis of lipoid pneumonia could be made mainly by the history and supported by the bronchoscopic and radiologic findings

The optimal treatment for lipoid pneumonia has not been well established yet, and most treatment modalities are based on case reports [1,4]. Treatment is primarily supportive and generally conservative, followed by the treatment of complications. Whole lung lavage, sometimes used in the treatment of patients with symptomatic pulmonary alveolar proteinosis, may also be therapeutic in treating lipoid pneumonia [17-18]. BAL should be performed weekly until the BAL fluid is nearly transparent and the cell count returns to a normal range, and as soon as the diagnosis of lipoid pneumonia is confirmed, to prevent pulmonary fibrosis and other complications. In our case, we did not perform whole lung lavage, but the oily, transparent, yellowish fluid that appeared in the right middle lobe bronchus was cleared after BAL, and the follow-up bronchoscopy confirmed the disappearance of the oily, transparent fluid. Although some reports suggest using systemic corticosteroids to slow the inflammatory response (Table 1) [2], its use in treating lipoid pneumonia is controversial [6,19-21]. Because of the delayed resolution of the pneumonia patch on chest radiograph and the inflammatory change in the bronchus noted on bronchoscopy, steroid was given to our patient, and his symptoms and the chest radiograph improved gradually. No special adverse effect was noted in our patient during the steroid therapy.

The natural history and outcome of lipoid pneumonia vary, depending on the type, volume, and distribution of the oil aspirated [1]. The majority of patients with an acute presentation have clinical and radiographic improvement after treatment, similar to the usual course of pneumonia. Our patient had both radiologic and clinical improvement, and no obvious complication was noted after proper treatment.

In conclusion, we reported an uncommon case of lipoid pneumonia that was treated successfully. In patients with pneumonia, especially those with delayed resolution of the pneumonia patch, the possibility of lipoid pneumonia should be considered; careful history-taking remains the keystone for a correct diagnosis.

References

1. Khilnani GC, Hadda V, *et al*. Lipoid pneumonia: an uncommon entity. Indian J Med Sci 2009; 63: 474-80.
2. Pielaszkiewicz-Wydra M, Homola-Piekarska B, Szczesniak E, *et al*. Exogenous lipoid pneumonia - a case report of a fire-eater. Pol J Radiol 2012; 77: 60-4.
3. Seaton A. Lipoid pneumonia in a fire breather. Occup Med (Lond) 2010; 60: 406.

Table 1. Steroid therapy used in lipoid pneumonia: comparison of recent reports

Authors, Year	Age/Sex	Image findings	Initial dosage of steroid	Duration of treatment
Chin, *et al*., 1994 [20]	40/Male	Mass lesion in the right lower lobe	Prednisolone 30 mg per day	3 months
Russo, *et al*., 2006 [21]	44/Female	Diffuse ground-glass opacity	Methylprednisolone 2 mg/kg/day	30 days
Hadda, *et al*., 2009 [6]	20/Male	Consolidation in the right middle and lower lobe	Hydrocortisone 300 mg per day, then prednisolone 60 mg per day	4 weeks
Lococo, *et al*., 2012 [22]	61/Male	Single pulmonary nodule	Prednisolone 60 mg per day	3 months
Indumathi, *et al*., 2012 [19]	2.5/Female	Bilateral opacities in the middle and lower lung zones	Prednisolone 2 mg/kg per day	18 weeks
Pielaszkiewicz-Wydra, *et al*., 2012 [2]	44/Male	Fat-fluid density in the lower part of the right middle lobe	Hydrocortisone 200 mg/day, then prednisolone 20 mg/day	3 months
Present case	46/Male	Consolidation in the right middle lobe	Prednisolone 30 mg per day	3 months

4. Hadda V, Khilnani GC, *et al*. Lipoid pneumonia: an overview. Expert Rev Respir Med 2010; 4: 799-807.
5. Simmons A, Rouf E, Whittle J, *et al*. Not your typical pneumonia: a case of exogenous lipoid pneumonia. J Gen Intern Med 2007; 22: 1613-6.
6. Hadda V, Khilnani GC, Bhalla AS, *et al*. Lipoid pneumonia presenting as non-resolving community acquired pneumonia: a case report. Cases J 2009; 2: 9332.
7. Marchiori E, Zanetti G, Mano CM, *et al*. Lipoid pneumonia in 53 patients after aspiration of mineral oil: comparison of high-resolution computed tomography findings in adults and children. J Comput Assist Tomogr 2010; 34: 9-12.
8. Betancourt SL, Martinez-Jimenez S, Rossi SE, *et al*. Lipoid pneumonia: spectrum of clinical and radiologic manifestations. AJR Am J Roentgenol 2010; 194: 103-9.
9. Haas C, Lebas FX, Le Jeunne C, *et al*. Pneumopathies caused by inhalation of hydrocarbons: apropos of 3 cases. Ann Med Interne (Paris) 2000; 151: 438-47.
10. Lee KS, Muller NL, Hale V, *et al*. Lipoid pneumonia: CT findings. J Comput Assist Tomogr 1995; 19: 48-51.
11. Chiang IC, Lin YT, Liu GC, *et al*. Exogenous lipoid pneumonia: serial chest plain roentgenography and high-resolution computerized tomography findings. Kaohsiung J Med Sci 2003; 19: 593-8.
12. Baron SE, Haramati LB, Rivera VT, *et al*. Radiological and clinical findings in acute and chronic exogenous lipoid pneumonia. J Thorac Imaging 2003; 18: 217-24.
13. Levade T, Salvayre R, Dongay G, *et al*. Chemical analysis of the bronchoalveolar washing fluid in the diagnosis of liquid paraffin pneumonia. J Clin Chem Clin Biochem 1987; 25: 45-8.
14. Colombo JL, Hallberg TK, *et al*. Recurrent aspiration in children: lipid-laden alveolar macrophage quantitation. Pediatr Pulmonol 1987; 3: 86-9.
15. Knauer-Fischer S, Ratjen F, *et al*. Lipid-laden macrophages in bronchoalveolar lavage fluid as a marker for pulmonary aspiration. Pediatr Pulmonol 1999; 27: 419-22.
16. Kazachkov MY, Muhlebach MS, Livasy CA, *et al*. Lipid-laden macrophage index and inflammation in bronchoalveolar lavage fluids in children. Eur Respir J 2001; 18:

790-5.

17. Sias SM, Daltro PA, Marchiori E, *et al*. Clinic and radiological improvement of lipoid pneumonia with multiple bronchoalveolar lavages. Pediatr Pulmonol 2009; 44: 309-15.
18. Ciravegna B, Sacco O, Moroni C, *et al*. Mineral oil lipoid pneumonia in a child with anoxic encephalopathy: treatment by whole lung lavage. Pediatr Pulmonol 1997; 23: 233-7.
19. Indumathi CK, Vikram KS, Paul P, *et al*. Severe lipoid pneumonia following aspiration of machine oil: successful treatment with steroids. Indian J Chest Dis Allied Sci 2012; 54: 197-9.
20. Chin NK, Hui KP, Sinniah R, *et al*. Idiopathic lipoid pneumonia in an adult treated with prednisolone. Chest 1994; 105: 956-7.
21. Russo R, Chiumello D, Cassani G, *et al*. Case of exogenous lipoid pneumonia: steroid therapy and lung lavage with an emulsifier. Anesthesiology 2006; 104: 197-8.
22. Lococo F, Cesario A, Porziella V, *et al*. Idiopathic lipoid pneumonia successfully treated with prednisolone. Heart Lung 2012; 41: 184-7.

以類固醇成功治療類脂性肺炎－病例報告與文獻回顧

阮懷磊 *　楊志仁 *,***,****　尹莘玲 **　王東衡 *,*****　黃吉志 *,*****　黃明賢 *,****

類脂性肺炎是由於肺部油脂堆積而造成的少見疾病。診斷的方式主要是依據臨床病史、影像學表現及支氣管肺泡灌洗液分析等。我們在此報告一名四十六歲男性在誤吸柴油後引發咳嗽、發燒及肋膜痛等症狀，入院時的胸部 X 光顯示右中下肺野實質性變化，故初步診斷為吸入性肺炎並投予抗生素治療。支氣管鏡檢查發現右中下肺葉分支有殘留的黃色油滴，但細胞學檢查及微生物培養皆無任何發現。抗生素治療後胸部 X 光仍無明顯改善，胸部電腦斷層顯示右中肺葉異質性密度的實質化病灶，而電腦斷層導引切片顯示壞死性發炎，追蹤支氣管鏡檢查顯示局部黏膜的發炎反應仍相當明顯。投予類固醇（Prednisolone 30 mg/day）治療後，追蹤顯示臨床症狀及胸部 X 光皆有明顯的改善，且無明顯的副作用或併發症。因此，對於類脂性肺炎的治療必須有詳細的病史及診斷，類固醇的使用可能有不錯的幫助。*(胸腔醫學 **2014; 29: 118-125**)*

關鍵詞：類脂性肺炎，肺炎，支氣管鏡

高雄醫學大學附設中和紀念醫院　內科部　胸腔內科 *，病理部 **
大同醫院內科 ***，醫學院醫學系 ****，醫學院呼吸治療學系 *****
索取抽印本請聯絡：黃明賢醫師，高雄醫學大學附設中和紀念醫院　內科部　胸腔內科，高雄市 807 自由一路 100 號